1 **Mtb specific HLA-E restricted T cells are induced during *Mtb* infection but not**
2 **after BCG administration in non-human primates and humans**

3 Linda Voogd[1], Marjolein van Wolfswinkel[1], Iman Satti[2], Andrew D. White[3], Karin Dijkman[4],

4 Anele Gela[5], Krista E. van Meijgaarden[1], Kees L.M.C. Franken[1], Julia L. Marshall[2], Tom H.M.

5 Ottenhoff[1], Thomas J. Scriba[5], Helen McShane[2], Sally A. Sharpe[3], Frank A.W. Verreck[4] and

6 Simone A. Joosten[1,*]

7   1. Leiden University Center for Infectious Diseases, Leiden University Medical Center,
8   Leiden, The Netherlands
9   2. The Jenner Institute, University of Oxford, Oxford, United Kingdom (UK)
10   3. UK Health Security Agency, Porton Down, UK
11   4. Biomedical Primate Research Centre, Rijswijk, The Netherlands
12   5. South African Tuberculosis Vaccine Initiative, Institute of Infectious Diseases and
13   Molecular Medicine and Division of Immunology, Department of Pathology, University
14   of Cape Town, Cape Town, South Africa

15   * Correspondence: s.a.joosten@lumc.nl

16

17 **Abstract**

18 Novel vaccines targeting the world's deadliest pathogen *Mycobacterium tuberculosis* (*Mtb*)

19 are urgently needed as the efficacy of the Bacillus Calmette–Guérin (BCG) vaccine in its

20 current use is limited. HLA-E is a virtually monomorphic unconventional antigen presentation

21 molecule and HLA-E restricted *Mtb* specific CD8⁺ T cells can control intracellular *Mtb* growth,

22 making HLA-E a promising vaccine target for *Mtb*. In this study, we evaluated the frequency

23 and phenotype of HLA-E restricted *Mtb* specific CD4⁺/CD8⁺ T cells in the circulation and

24 bronchoalveolar lavage fluid of two independent non-human primate (NHP) studies and from

25 humans receiving BCG either intradermally or mucosally. BCG vaccination followed by *Mtb*

26 challenge in NHPs did not affect the frequency of circulating and local HLA-E/*Mtb* CD4⁺ and

27 CD8⁺ T cells, and we saw the same in humans receiving BCG. HLA-E/*Mtb* T cell frequencies

28 were significantly increased after *Mtb* challenge in unvaccinated NHPs, which was correlated

29 with higher TB pathology. Together, HLA-E/*Mtb* restricted T cells are minimally induced by

30 BCG in humans and rhesus macaques (RMs) but can be elicited after *Mtb* infection in

31 unvaccinated RMs. These results give new insights into targeting HLA-E as a potential

32 immune mechanism against TB.

33 **Key words:** HLA-E; Vaccine; BCG; Tuberculosis; T cells

34

1. Introduction

Tuberculosis (TB) disease, caused by infection with *Mycobacterium tuberculosis* (*Mtb*), is a significant global health problem accounting for more than a million deaths each year[1]. Bacillus Calmette–Guérin (BCG) is the only licensed vaccine to protect against TB, however it has poor efficacy in adults in its current use. There is an urgent need for better protective vaccines against TB. Non-human primates (NHPs), specifically cynomolgus and rhesus macaques (CMs and RMs), are arguably the best pre-clinical models to evaluate novel vaccine strategies against TB and to increase our understanding of lung mucosal immune responses against *Mtb*. NHPs can develop the same pathology as human TB disease, including the formation of lung granulomas, lymph node involvement and the occurrence of latency[2,3].

Donor-unrestricted T cells (DURTs) recognize non-polymorphic antigen presentation molecules and most DURT subsets express invariant T cell receptors (TCRs)[4]. Vaccination approaches targeting DURTs can thus potentially induce protection irrespective of the genetic diversity in the human population. HLA-E restricted T cells belong to the DURT family because humans express two functional HLA-E alleles, HLA-E*01:01 and *01:03, that only differ in one amino acid located outside the peptide binding groove. This limited diversity suggests that both alleles have a comparable peptide binding repertoire[5,6]. HLA-E was first discovered as a ligand for the CD94/NKG2A(C) co-receptor inhibitory complex expressed on Natural Killer cells, which is an important surveillance mechanism to scan for, and subsequently clear, cells with defects in their antigen presentation machinery[7-9]. TCRs can also recognize HLA-E/peptide complexes[10] and HLA-E restricted CD8+ T cells have been identified in the circulation in patients with malignancies and infections, as we have shown previously in active TB (aTB) or *Mtb* infected (TBI) individuals with and without HIV co-infection[11-13]. Individuals with concomitant aTB and HIV infection demonstrated the highest frequency of circulating HLA-E restricted *Mtb* specific CD8+ T cells and revealed an unorthodox phenotype characterized by the secretion of T-helper 2 (Th2) associated cytokines, cytolysis of HLA-E/*Mtb* presenting target cells and inhibition of intracellular *Mtb* growth in *Mtb*-infected macrophages[13-22]. Moreover, in the absence of Qa-1b, the mouse equivalent of HLA-E, mice succumbed earlier from *Mtb* infection, suggesting a possible functional role of HLA-E in host defence[23].

The potential of HLA-E as a target for vaccination has been illustrated previously in RMs vaccinated with strain 68-1 rhesus cytomegalovirus (RhCMV) vectors encoding SIV antigens (called 68-1 RhCMV/SIV)[24]. Vaccination with this vector inhibited SIV replication and cleared SIV infection in more than half of the vaccinated RMs[25]. Importantly, the induction of MHC-E restricted CD8+ T cells following vaccination was essential to establish

70   this protective effect[25,26]. Besides its virtual monomorphism, another advantage of targeting

71   HLA-E by vaccination is that HLA-E is not downregulated upon HIV co-infection, in contrast to

72   classical HLA-I molecules, which is an important benefit as infection with HIV and TB

73   significantly overlap in endemic areas[27]. Together, these findings illustrate the potential for

74   targeting HLA-E restricted T cells as a vaccination strategy against TB.

75   As individuals in TB endemic areas are routinely vaccinated with BCG, we sought to

76   determine if HLA-E restricted *Mtb* specific T cells are induced in the circulation and

77   bronchoalveolar lavage (BAL) fluid following BCG and/or *Mtb* challenge in two NHP studies

78   and in humans after receiving BCG either intradermally (ID) or by aerosol. If induced, HLA-E

79   might be a promising target to induce *de novo* T cell responses in BCG vaccinated individuals.

80   Our results show that HLA-E/*Mtb* CD4$^+$ and CD8$^+$ T cell frequencies remained stable in the

81   circulation of humans after receiving BCG, and in the BAL and circulation of BCG vaccinated

82   and *Mtb* challenged RMs. Frequencies were increased in the BAL of unvaccinated and *Mtb*

83   challenged RMs. These findings expand our knowledge on the induction of HLA-E restricted

84   T cells after receiving BCG and upon *Mtb* infection in both the periphery as well as at the local

85   site of infection.

86

87   **2. Material and Methods**

88   *2.1 HLA-E TM folding and production*

89   HLA-E*01:01 and *01:03 tetramers (TMs) were produced and correct folding of the monomers

90   with the peptides was confirmed by staining LILRB1 expressing cells and mass spectrometry,

91   as described previously[28]. Table 1 shows the HLA-E TMs used in each study.

92

93   **Table 1.** Overview of the HLA-E *Mtb* and CMV derived peptide (pools) used for HLA-E TM staining on
94   PBMC and BAL samples in the human BCG revaccination and infection studies, RM studies 1 and 2
95   and the CM study.

Peptide name	Sequence	Allele	Fluorochrome
Human BCG infection studies 1 and 2: *Mtb* pool and CMV			
p34	VMTTVLATL	HLA-E*01:01 + HLA-E*01:03 separately	PE
p55	VMATRRNVL	HLA-E*01:01 + HLA-E*01:03 separately	PE
p62	RMPPLGHEL	HLA-E*01:01 + HLA-E*01:03 separately	PE
p68	VLRPGGHFL	HLA-E*01:01 + HLA-E*01:03 separately	PE
pCMV	VLAPRTLLL	HLA-E*01:01 + HLA-E*01:03 separately	APC
Human BCG revaccination study: *Mtb* pool and CMV			
p34	VMTTVLATL	HLA-E*01:01 + HLA-E*01:03 combined	PE

p55	VMATRRNVL	HLA-E*01:01 + HLA-E*01:03 combined	PE
p62	RMPPLGHEL	HLA-E*01:01 + HLA-E*01:03 combined	PE
p68	VLRPGGHFL	HLA-E*01:01 + HLA-E*01:03 combined	PE
pCMV	VLAPRTLLL	HLA-E*01:01 + HLA-E*01:03 combined	APC
NHP studies: *Mtb* pool 1			
p55	VMATRRNVL	HLA-E*01:03	PE
p62	RMPPLGHEL	HLA-E*01:03	PE
NHP studies: *Mtb* pool 2			
MTBHLAE_31	VLPAKLILM	HLA-E*01:03	PE
MTBHLAE_34	LLPIKIPLI	HLA-E*01:03	PE
MTBHLAE_63	ILAFEAPEL	HLA-E*01:03	PE
MTBHLAE_93	RLEAVVMLL	HLA-E*01:03	PE
NHP studies: CMV			
pCMV	VLAPRTLLL	HLA-E*01:03	PE
NHP studies: p44			
p44	RLPAKAPLL	HLA-E*01:03	PE

2.2 Human BCG revaccination study

Eighty-two participants of a TBRU-supported BCG revaccination trial were enrolled at the South African Tuberculosis Vaccine Initiative, Cape Town, South Africa[29,30]. This trial was approved by the Medicines Control Council (MCC) of South Africa (now called South African Health Products Regulatory Authority, SAHPRA), by the University Hospital Cleveland Medical Center Institutional Board and the Human Research Ethics Committee of the University of Cape Town (387/2008). Written informed consent was obtained from all participants. The TBRU cohort comprised healthy tuberculin skin test positive, HIV uninfected adults who received routine BCG vaccination at birth. Participants were randomly assigned to two groups. Group 1 received at least six months of Isoniazid preventive therapy (IPT) before intradermal BCG revaccination and group 2 received IPT six months after intradermal BCG revaccination. Samples from twenty individuals of group 1 were used in the current study. Peripheral blood mononuclear cells (PBMCs) were collected and cryopreserved before BCG revaccination and 3, 5 and 52 weeks after BCG revaccination (Figure S1A for study overview). Cryopreserved PBMCs were thawed in pre-warmed (37°C) media containing DNAse (Sigma-Aldrich) and were washed in PBS. PBMCs were then stained with LIVE/DEAD™ Fixable Near-IR Dead Cell Stain (Invitrogen) (1:1000 in PBS) for 20 min at room temperature (RT) in the dark. PBMCs were again washed in PBS and blocked with 12.5 µg/mL purified anti-CD94 antibody (BD Bioscience) followed by another wash in PBS/0.1% BSA. PBMCs were then

117   stained with a pool of HLA-E*01:01 and *01:03 TMs (0.4 μg/TM) folded with the peptides

118   shown in Table 1 for 15 min at 37°C in the dark. PBMCs were washed in PBS/0.1% BSA and

119   were stained with APC-H7 CD14 (clone MOP9, BD Bioscience), APC-H7 CD19 (clone SJ25-

120   C1, BD Bioscience), AlexaFluor700 CD3 (clone UCHT1, BioLegend), BV510 CD4 (clone RPA-

121   T4, BioLegend), BV785 CD8 (clone SK1, BioLegend), BV605 CD26 (clone L272, BD

122   Bioscience), BV650 CD161 (clone DX12, BD Bioscience), PE-Cy7 TRAV1.2 (clone 3C10,

123   BioLegend), PE-Cy5 HLA-DR (clone L243, BioLegend), BV711 $\gamma\delta$ TCR (clone B1, BD

124   Bioscience), PE-CF594 CCR7 (clone 3D12, BD Bioscience) and PerCP-eFluor710 CD45RA

125   (clone HI100, BioLegend) with pre-defined dilutions in BD Brilliant Stain Buffer (BD

126   Bioscience) for 20 min at 4°C in the dark. PBMCs were washed in PBS/0.1% BSA, fixated in

127   1% paraformaldehyde, and acquired on a BD LSR-II flow cytometer. The gating strategy to

128   determine HLA-E CD4$^+$ and CD8$^+$ T cell frequencies and their phenotype is shown in Figure

129   S2A.

130

131   *2.3 Controlled human BCG infection studies 1 and 2*

132   Two controlled human BCG infection studies were performed at the University of Oxford (UK).

133   The trial protocol of the first BCG controlled human infection study was approved by the

134   Medicines and Healthcare products Regulatory Agency (EudraCT: 2015-004981-27) and the

135   South-Central Oxford A Research Ethics Committee (REC) (15/SC/0716). Twelve BCG-naïve

136   UK adults received the BCG Bulgaria strain (InterVax Ltd.) via aerosol inhalation of 1×10^7

137   Colony Forming Units (CFU) using an Omron MicroAir mesh nebuliser and twelve adults via

138   standard intradermal injection of 1×10^6 CFU[31]. Blood was taken from all twenty-four

139   volunteers at the start and seven and fourteen days after infection (Figure S1B for study

140   overview). The trial protocol of the second aerosol BCG infection study was approved by the

141   Central Oxford A REC (18/SC/0307) and is registered at ClinicalTrials.gov (NCT03912207).

142   Six healthy BCG-naïve UK adults received the BCG Danish strain (AJVaccine) via aerosol

143   inhalation of 1×10^7 CFU using an Omron MicroAir mesh nebuliser. Bronchoalveolar lavage

144   (BAL) and blood were taken fourteen days after receiving BCG from all individuals (Figure

145   S1C for study overview). PBMCs were isolated and cryopreserved. Flow cytometric analysis

146   was performed after thawing the PBMC samples whereas BAL samples were directly stained

147   upon collection and isolation. BAL and PBMC (3×10^6 cells each) were stained (1×10^6 cells /

148   well) with fixable LIVE/DEAD™ Vivid (Thermofisher) for 10 min at 40°C. Samples were then

149   blocked with purified αCD94 (clone HP-3D9, BD Biosciences) and were stained with either:

150   HLA-E*01:01, HLA-E *01:03 and CMV control TMs (Table 1) or left unstained to serve as

151   gating control for TMs. Cells were incubated for 15 min at 37°C and were then washed before

152   adding the surface staining antibody mix. The following antibodies were added to all cells:
153   CD3-AF700 (Clone UCHT1, Thermofisher), CD4-FITC (Clone: RPA-T4, BioLegend), CD8-
154   APC/H7 (Clone SK1, BD Bioscience), CD14-Pacific blue (Thermofisher) and CD19-Pacific
155   blue (Thermofisher). Cells were incubated with the surface antibody mix for 30 min at 4°C and
156   were then washed before being acquired on LSR Fortessa v.2 Std X20 flow cytometer using
157   BD FACSDiva 8.0.2 and the data was analysed on FlowJo v9. The gating strategy to
158   determine HLA-E CD4$^+$ and CD8$^+$ T cell frequencies in human PBMC and BAL for studies 1
159   and 2 is shown in Figure S2B.

160

161   *2.4 Rhesus macaque study 1: Ethics, animal care, vaccination and pathology assessment*

162   Archived samples from the study published by White *et al.* were used in the current study[32].
163   Study design and animal welfare procedures were approved by the UK Health Security
164   Agency Animal Welfare and Ethical Review Body and was authorised under UK Home Office
165   Licence P219D8D1A. Nineteen healthy Indian-type rhesus macaques (*Macaca mulatta*) from
166   a closed UK breeding colony were housed in groups in accordance with the UK Home Office
167   Code of Practice and NC3Rs guidelines on Primate Accommodation. Six animals received the
168   BCG Danish strain 1331 via intradermal injection into the upper left arm and six animals
169   received BCG by aerosol exposure using an Omron MicroAir mesh nebuliser with an
170   estimated dose of 2-8x10^6 CFU/mL. The control group consisted of seven unvaccinated
171   animals. Twenty-one weeks after BCG vaccination, all animals were challenged with a
172   calculated single ultra-low dose of 3 CFU *Mtb* Erdman K01 via aerosol delivery. The apparatus
173   and procedure for aerosol delivery of *Mtb*, including the calculation of the presented dose were
174   performed as described previously[32]. Blood from all RMs was collected and PBMCs were
175   cryopreserved. Samples at the time points shown in Figure S1D were shipped to the LUMC,
176   The Netherlands for flow cytometry analysis. PBMCs were thawed for staining with HLA-
177   E*01:03 TMs folded with *Mtb* pool 1 and pool 2, p44 and CMV (Table 1) and cell surface
178   markers as outlined in detail below. Samples were acquired on a BD FACS Lyric 3L12C (BD
179   Biosciences).

180

181   *2.5 Rhesus macaque study 2: Ethics, animal care, vaccination, and pathology assessment*

182   Archived samples from the study published by Dijkman *et al.* were used in the current
183   study[33]. Ethical approval of the study protocol was obtained from the independent ethics
184   committee Dier Experimenten Commissie (DEC) (761subB) and the institutional animal

185   welfare body of the Biomedical Primate Research Center (BPRC). The approved housing and
186   animal care procedures are described previously[33]. Twenty-four healthy male Indian-type
187   rhesus macaques (*Macaca mulatta*) from the in-house breeding colony were stratified into
188   three groups of eight animals. BCG vaccination or placebo was randomly assigned to each
189   group. Two of the three groups received between $1.5-6.0 \times 10^5$ CFU of the BCG strain Sofia
190   (InterVax Ltd.), either via intradermal injection or via endobronchial instillation (referred to as
191   mucosal vaccination) into the lower left lung lobe. Animals receiving saline via endobronchial
192   instillation served as the control group. Twelve weeks after BCG vaccination or saline
193   treatment all animals received a weekly calculated limiting dose of 1 CFU *Mtb* Erdman K01
194   strain for eight consecutive weeks. Infection was confirmed with IFN-γ ELISpot. Blood and
195   BAL samples were collected, PBMCs and BAL cells were isolated and cryopreserved.
196   Samples at the time points shown in Figure S1E were shipped to the LUMC, The Netherlands.
197   PBMCs and BAL cell samples were thawed for staining with HLA-E*01:03 TMs folded with
198   *Mtb* pool 1 and pool 2, p44 and CMV (Table 1) and cell surface markers as outlined in detail
199   below. Samples were acquired on a BD FACS Lyric 3L12C (BD Biosciences). Bacterial loads
200   (i.e., CFU counts) in lung tissues and post-mortem pathology scores (i.e., lesion size and
201   granuloma formation) were determined at the BPRC.

202

203   *2.6 Cynomolgus macaque study: Ethics, animal care, vaccination and pathology assessment*

204   Archived samples from the study published by White *et al.* were used in the current study[34].
205   Study design and animal housing was approved by the Establishment Animal Welfare and
206   Ethical Review Committee and authorised under UK Home Office Project License
207   P219D8D1A. The approved housing and animal care procedures are described previously[34].
208   Nine cynomolgus macaques (*Macaca fascicularis*) from a closed UK breeding colony were
209   stratified into three groups of three animals. One group received between $2-8 \times 10^5$ CFU/mL
210   BCG Danish strain 1331 via intradermal injection into the upper left arm. Twenty-one weeks
211   after vaccination all animals were challenged with a calculated dose of 5 CFU *Mtb* Erdman
212   strain K01 via aerosol delivery. Sixteen weeks after *Mtb* challenge, all groups were challenged
213   with $106-107$ $(TCID)_{50}$ SIVmac32H 11/88. Infection with SIV was confirmed via culturing
214   PBMCs with C8166 cells to examine the cytopathic effect. Blood from all animals was
215   collected, and PBMCs were isolated and cryopreserved at the time points shown in Figure
216   S1F. Cryopreserved PBMCs were shipped to the LUMC, The Netherlands for flow cytometry
217   analysis. PBMCs were thawed for staining with HLA-E*01:03 TMs folded with *Mtb* pool 1 and
218   2, p44 and CMV (Table 1) and cell surface markers as outlined in detail below. Samples were
219   acquired on a BD FACS Lyric 3L12C (BD Biosciences).

220

2.7 Flow cytometry staining, acquisition and analysis of NHP PBMC and BAL samples

NHP samples were processed at the Biosafety Level 3 (BSL3) laboratory at the LUMC, The Netherlands. PBMC and BAL samples were thawed and rested for 2 hrs in PBS with 0.2 mg/mL DNase I (Roche Diagnostics GmbH) at 37°C with 5% CO_2 to adhere monocytic cells. Cells were washed (10 min, 450 x g) and stained using previously developed and optimized staining procedures for high dimensional flow cytometry panels[35]. Samples were stained with LIVE/DEAD™ Fixable Violet (Invitrogen) according to manufacturer's instructions in PBS for 30 min at room temperature (RT) in the dark. Cells were then washed (5 min, 450 x g) with PBS, blocked with 5% pooled normal human serum in PBS for 10 min at RT to block Fc receptors and prevent non-specific binding and washed once with PBS/0.1% BSA. Cells were subsequently stained with an antibody cocktail containing True-Stain Monocyte Blocker (1:20, BioLegend) to block non-specific binding of tandem dyes to monocytes, Brilliant Stain Buffer Plus (1:10, BD Biosciences) and the chemokine receptor antibodies PE-Cy7 CCR4 (1:100, clone 1G1, BD Biosciences), BV605 CCR6 (1:100, clone 11A9, BD Biosciences), BV785 CCR7 (1:50, clone G043H7, BioLegend) and APC-Cy7 CXCR3 (1:50, clone G025H7, BioLegend) in PBS/0.1% BSA for 30 min at 37°C in the dark. After incubation, cells were washed once with PBS/0.1% BSA and incubated with the HLA-E*01:03 TM conditions (5.4 µg/mL per TM) shown in Table 1 in PBS/0.1% BSA for 30 min at 37°C in the dark. Peptide p44 is a high affinity *Mtb*-derived HLA-E restricted peptide that adopts a similar conformation in the peptide binding groove as classical HLA-I leader sequence derived peptides[36] and served as a control. Cells were then washed once with PBS/0.1% BSA, fixated with 1% paraformaldehyde (Pharmacy LUMC, Leiden) for 10 min at RT and washed with PBS/0.1% BSA. Cells were subsequently stained with an antibody cocktail containing Brilliant Stain Buffer Plus (1:10) and the surface antibodies BV421 CD14 (1:100, clone M5E2, BD Biosciences) and BV421 CD19 (1:200, clone 2H7, BD Biosciences) as dump channel together with the LIVE/DEAD stain, PerCP-Cy5.5 CD3 (1:25, clone SP34-2, BD Biosciences), R718 CD4 (1:50, clone L200, BD Biosciences), FITC CD8 (1:50, clone SK1, BD Biosciences), BV510 CD45RA (1:200, clone 5H9, BD Biosciences), BV711 CD16 (1:100, clone 3G8, BD Biosciences) and APC NKG2A (1:100, clone Z199, Beckman Coulter) in PBS/0.1% BSA for 30 min at 4°C in the dark. For the BAL samples, because of high autofluorescence, BV605 CD8 (1:100, clone SK1, BD Biosciences) was used instead of FITC CD8 and therefore CCR6 was not included in the BAL sample analysis. After incubation, cells were washed twice with PBS/0.1% BSA, fixated with 1% paraformaldehyde for 10 min at RT and washed twice with PBS/0.1% BSA. Cells were then resuspended in PBS/0.1% BSA and acquired on a BD FACS

255   Lyric 3L12C (BD Biosciences). Flow cytometry data was analysed using FlowJo v10.9.0.

256   Subsequent (statistical) analysis was performed in GraphPad Prism v9.3.1. The gating

257   strategy to determine HLA-E CD4$^+$ and CD8$^+$ T cell frequencies and their phenotype in PBMC

258   and BAL samples are shown in Figure S3A and B, respectively.

259

260   **3   Results**

261   *3.1 The frequency of circulating HLA-E/Mtb CD4$^+$ and CD8$^+$ T cells remains stable in*

262   *humans and RMs after receiving BCG*

263   The frequency of circulating HLA-E/*Mtb* CD4$^+$ and CD8$^+$ T cells remained stable after

264   intradermal BCG revaccination in healthy adults (Figure 1A), similar to the stability observed

265   in BCG naïve humans receiving primary intradermal or aerosol BCG (Figure 1B). BCG

266   administered as a boost or prime therefore did not induce HLA-E/*Mtb* CD4$^+$ and CD8$^+$ T cells

267   in humans.

268   Representative density plots for p44 (negative control), CMV and *Mtb* pool 1 and 2

269   before and after BCG vaccination in RMs are shown in Figure S4A and B, respectively. The

270   frequency of circulating HLA-E/*Mtb* CD4$^+$ and CD8$^+$ T cells was unchanged post-BCG

271   vaccination compared to pre-vaccination in both RM study 1 and 2 with no differences

272   observed between administration routes (Figure 1C and D). HLA-E CMV TMs were only

273   recognized by CD8$^+$ T cells, whereas HLA-E/*Mtb* TMs were recognized by both CD4$^+$ and

274   CD8$^+$ T cells in RMs and the recognition between CD4$^+$ and CD8$^+$ HLA-E/*Mtb* T cells was

275   strongly correlated in both humans and RMs (Figure 1E). The frequency of HLA-E/CMV CD8$^+$

276   T cells in the circulation was overall higher compared to HLA-E/*Mtb* CD4$^+$ and CD8$^+$ T cells

277   (10% vs. 0.3%). Combined, BCG administration in RMs did not increase the frequency of HLA-

278   E/*Mtb* T cells in the circulation irrespective of the administration route.

279
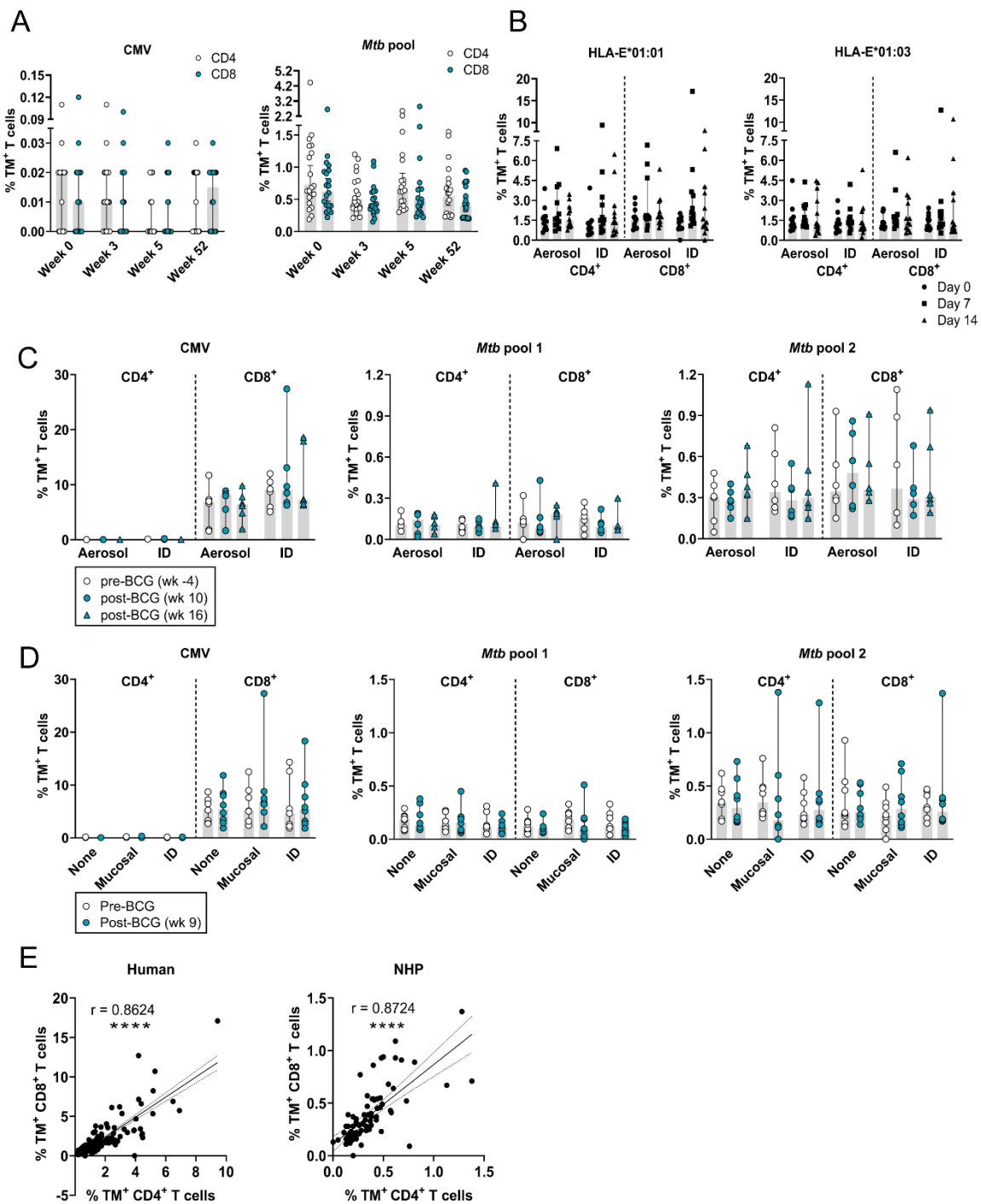
Figure 1. HLA-E/*Mtb* and CMV CD4+ and CD8+ T cell frequencies in the circulation remain stable after receiving BCG in humans and RMs. Peptide pools for HLA-E TM staining on human and RM samples are shown in Table 1. **(A)** HLA-E*01:03 and *01:01 CD4+ and CD8+ T cell frequencies for CMV (left) and the *Mtb* pool (right) at week 0 and 3, 5 and 52 weeks after intradermal BCG revaccination in healthy TST+ HIV- volunteers (n=20); **(B)** HLA-E*01:01 (left) and *01:03 (right) CD4+ and CD8+ T cell frequencies for the *Mtb* pool on day 0 (circles) and 7 (squares) and 14 (triangles) days after aerosol BCG inhalation (n=12) or intradermal BCG administration (n=12) in healthy volunteers; **(C)** HLA-E*01:03 CD4+ and CD8+ T cell frequencies for CMV (left), *Mtb* pool 1 (middle) and 2 (right) in RM study

288   1 at the pre-vaccination time point (white circles), 10 (blue circles) and 16 weeks post-vaccination (blue

289   triangles); **(D)** Same as C, but then for RM study 2 at the pre-vaccination time point (white circles) and

290   9 weeks post-vaccination (blue circles); **(E)** Correlating HLA-E CD4$^+$ T cell frequencies (X-axis) and

291   HLA-E CD8$^+$ T cell frequencies (Y-axis) at all time points in the human studies for the *Mtb* pool (left) and

292   in RM study 1 and 2 combined for *Mtb* pool 2 (right). Shaded bars represent the median frequency, and

293   the error bars represent the 95% confidence interval. Significance was tested using a repeated

294   measures (RM) two-way ANOVA with multiple comparison correction (A-D) and a Spearman's rank

295   correlation (E). * = $p<0.05$, ** = $p<0.01$, **** = $p<0.0001$.

296

297   *3.2 The frequency of circulating HLA-E/Mtb CD4$^+$ and CD8$^+$ T cells does not change after*

298   *Mtb challenge in unvaccinated and BCG vaccinated RMs*

299   Representative density plots for *Mtb* pool 2 (which shares the same recognition profile as *Mtb*

300   pool 1; see Figure S5 for results on *Mtb* pool 1) on pre- and post-*Mtb* challenge samples from

301   one aerosol BCG vaccinated RM are shown in Figure S4C. *Mtb* challenge with or without prior

302   BCG vaccination did not affect the frequency of circulating HLA-E/*Mtb* CD4$^+$ and CD8$^+$ T cells

303   in both RM studies and no differences were observed between the BCG administration routes

304   (Figure 2A and B). As such, the frequency of circulating HLA-E/*Mtb* CD4$^+$ and CD8$^+$ T cells

305   was not changed after *Mtb* challenge only or following BCG vaccination in RMs.
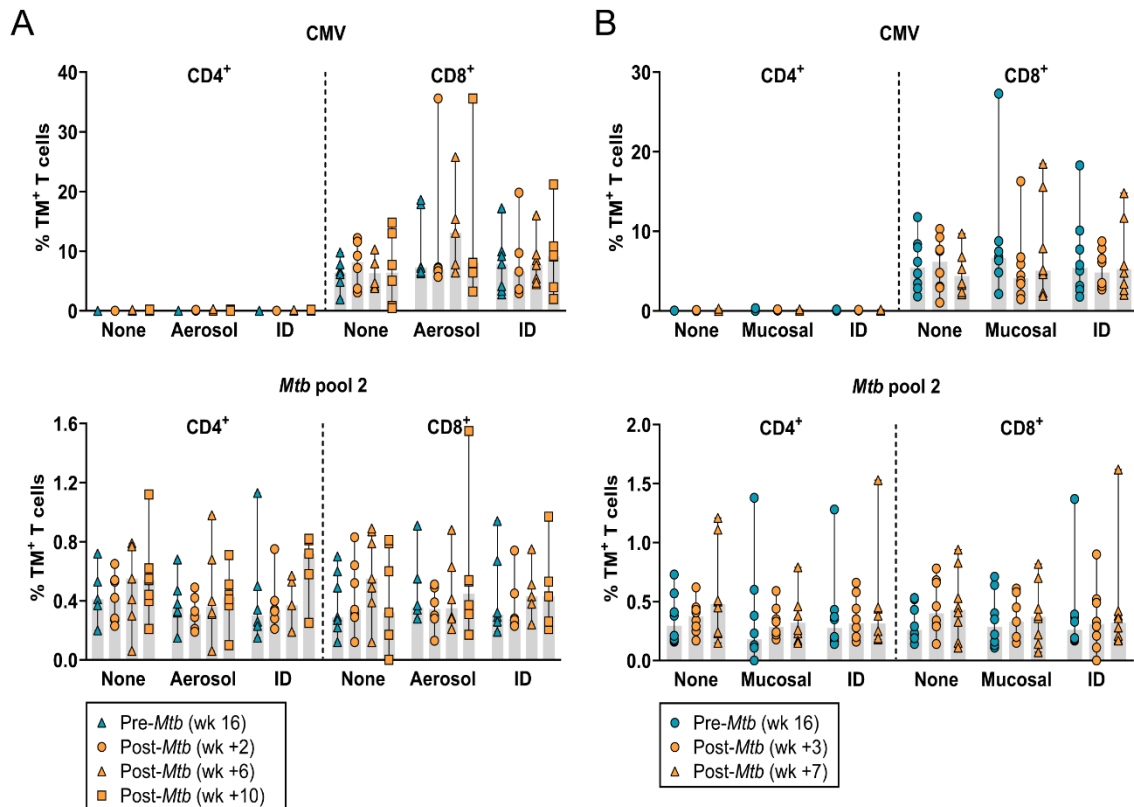
Figure 2. *Mtb* challenge only or following BCG vaccination in RMs results in stable HLA-E/*Mtb* and CMV CD4+ and CD8+ T cell frequencies in the circulation. Peptide pools for HLA-E TM staining on RM samples are shown in Table 1. **(A)** HLA-E*01:03 CD4+ and CD8+ T cell frequencies for CMV (upper panel) and *Mtb* pool 2 (lower panel) in RM study 1 at the pre-challenge time point (blue triangles) and 2 (orange circles), 6 (orange triangles) and 10 weeks (orange squares) post-*Mtb* challenge; **(B)** Same as A, but then in RM study 2 at the pre-challenge time point (blue circles) and 3 (orange circles) and 7 weeks (orange triangles) post-*Mtb* challenge. Shaded bars represent the median frequency, and the error bars represent the 95% confidence interval. Significance was tested using a repeated measures (RM) two-way ANOVA with multiple comparison correction. * = *p*<0.05, ** = *p*<0.01, **** = *p*<0.0001.

3.3 Increased frequency of HLA-E/Mtb CD4+ and CD8+ T cells in the BAL after Mtb challenge in unvaccinated RMs

Representative density plots for p44, CMV, *Mtb* pool 1 and 2 in the BAL from an unvaccinated RM after *Mtb* challenge are shown in Figure 3A. Both in RMs and humans, the frequency of HLA-E/*Mtb* CD4+ and CD8+ T cells was significantly higher in the BAL compared to the circulation, including for HLA-E/CMV CD8+ T cells in RMs (Figure 3B and C). Similar as in the circulation, the frequency of HLA-E/CMV CD8+ T cells was higher than HLA-E/*Mtb* CD4+ and CD8+ T cells in the BAL (Figure 3B). In contrast to BCG vaccination, *Mtb* challenge markedly and significantly increased the frequency of HLA-E/*Mtb* CD4+ and CD8+ T cells in the BAL of

326
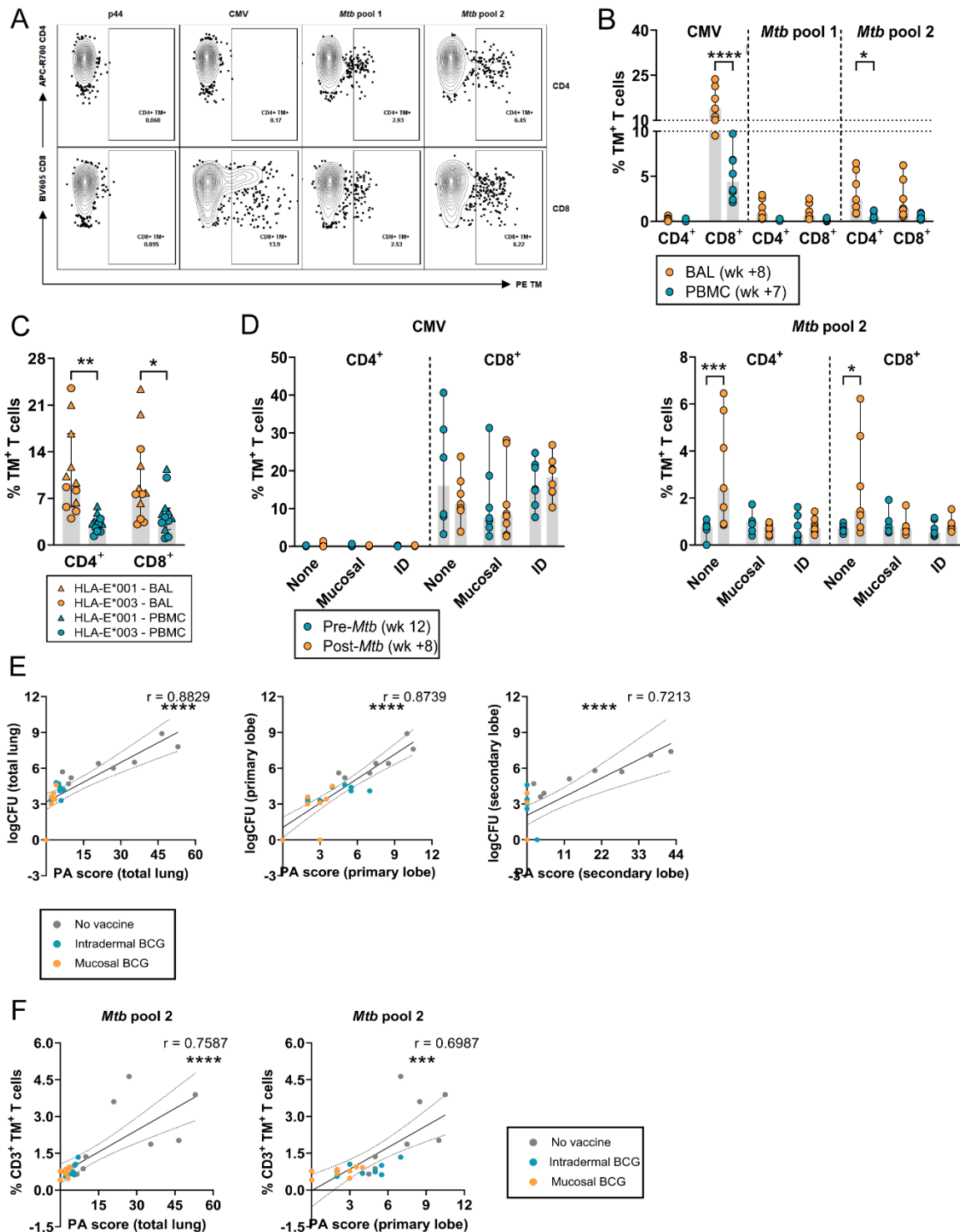
Figure 3. HLA-E/*Mtb* and CMV CD4+ and CD8+ T cell frequencies are increased after *Mtb* challenge in BAL of BCG unvaccinated RMs. Peptide pools for HLA-E TM staining on RM and human samples are shown in Table 1. **(A)** Density plots for HLA-E p44, CMV and *Mtb* pool 1 and 2 CD4+ and CD8+ T cell frequencies in a BAL sample of one representative unvaccinated RM of study 2 post-*Mtb* challenge. HLA-E TMs in PE are shown on the X-axis and CD4 and CD8 are shown on the Y-axis; **(B)** HLA-E*01:03 CD4+ and CD8+ T cell frequencies for CMV and *Mtb* pool 1 and 2 in BAL (orange) and PBMCs (blue), 8 and 7 weeks, respectively, post-*Mtb* challenge in unvaccinated RMs of RM study 2 (n=8); **(C)**

334   HLA-E*01:01 (triangles) and *01:03 (circles) CD4$^+$ and CD8$^+$ T cell frequencies in BAL (orange) and in

335   PBMCs (blue) for the *Mtb* pool, 14 days after aerosol BCG inhalation in healthy volunteers (n=12); **(D)**

336   HLA-E*01:03 CD4$^+$ and CD8$^+$ T cell frequencies in BAL for CMV (left) and *Mtb* pool 2 (right) in RM study

337   2, 12 weeks post-BCG vaccination (blue) and 8 weeks post-*Mtb* challenge (orange); **(E)** Correlating the

338   CFU counts (Y-axis) and the PA scores (X-axis) in the total lung (left), primary lobe (middle) and

339   secondary lobe (right) for RM study 2. Grey dots represent the unvaccinated group, blue dots the

340   intradermal BCG vaccinated group, and orange dots the mucosal BCG vaccinated group. Dotted lines

341   represent the 95% confidence interval; **(F)** Same as E, but then correlating HLA-E*01:03 *Mtb* CD3$^+$ T

342   cell frequencies in BAL (Y-axis) and the PA scores in the total lung (left) and primary lobe (right) (X-

343   axis) 8 weeks post-*Mtb* challenge. Shaded bars represent the median frequency, and the error bars

344   represent the 95% confidence interval. Significance was tested using a repeated measures (RM) two-

345   way ANOVA with multiple comparison correction (A-D) and a Spearman's rank correlation (E-F). * =

346   $p<0.05$, ** = $p<0.01$, **** = $p<0.0001$.

347

348   unvaccinated RMs (Figure 3D). There was a positive and significant correlation between the

349   PA scores and CFU counts in the lung, primary and secondary lobe of all RMs, which was

350   most pronounced in unvaccinated RMs (Figure 3E). HLA-E/*Mtb* CD3$^+$ T cell frequencies in the

351   BAL and the PA scores in the total lung and primary lobe were significantly correlated as well

352   (Figure 3F), which suggests that BCG vaccination can contribute to protection, reflected by

353   the lower PA scores in the vaccinated RMs, but likely by other mechanism than HLA-E, if

354   increased frequencies of HLA-E/*Mtb* restricted T cells is required for protection.

355

356   *3.4 HLA-E/Mtb CD3$^+$ T cells have a similar memory phenotype but altered chemokine*

357   *receptor expression compared to total T cells*

358   Circulating HLA-E/*Mtb* CD4$^+$ and CD8$^+$ T cells had a similar distribution of memory subsets

359   compared to total T cells in both RM studies, which was not changed upon BCG vaccination

360   or *Mtb* challenge (Figure 4A and B). In contrast, HLA-E/CMV CD8$^+$ T cells had a dominant

361   effector memory (EM) and terminally differentiated (EMRA) phenotype that did not change

362   after BCG vaccination and *Mtb* challenge in both RM studies (Figure 4A and B). Both CD4$^+$

363   and CD8$^+$ T cells can recognize HLA-E/*Mtb* (Figure 1E), therefore CCR expression was

364   evaluated on CD3$^+$ T cells. HLA-E/*Mtb* T cells had a significantly higher expression of CCR4

365   and lower expression of CXCR3 compared to HLA-E/CMV T cells and a higher expression of

366   CXCR3 compared to total T cells post-BCG vaccination (RM study 1 in Figure 4C and RM

367   study 2 in 4D). The expression of CCR6 was similar on HLA-E/CMV, HLA-E/*Mtb* T cells and

368   total T cells in RM study 1 (Figure 4C), but significantly increased on HLA-E/CMV T cells

369   compared to HLA-E/*Mtb* T cells in RM study 2 (Figure 4D). Similar findings for CCR expression

370   were found in the BAL, although the overall expression of CXCR3 was higher in the BAL

371   compared to the circulation (Figure 4E). Whereas the expression of CCR4, CCR6 and CXCR3

372   on HLA-E/*Mtb* T cells in the circulation and the BAL did not change upon *Mtb* challenge in

373   unvaccinated and vaccinated RMs (Figure 4F, G and H), HLA-E/CMV T cells in unvaccinated

374   RMs in study 2 had decreased expression of CXCR3 and CCR6 in the circulation and of

375   CXCR3 in the BAL after *Mtb* challenge compared to vaccinated RMs (Figure 4G and H). These

376   findings reveal that (i) BCG vaccination followed by *Mtb* challenge did not change the memory

377   phenotype of HLA-E/*Mtb* T cells in the circulation and that (ii) HLA-E/*Mtb* T cells have different

378   CCR expression levels compared to HLA-E/CMV T cells and total T cells, suggesting

379   pathogen specific expression.

380

381

382

383
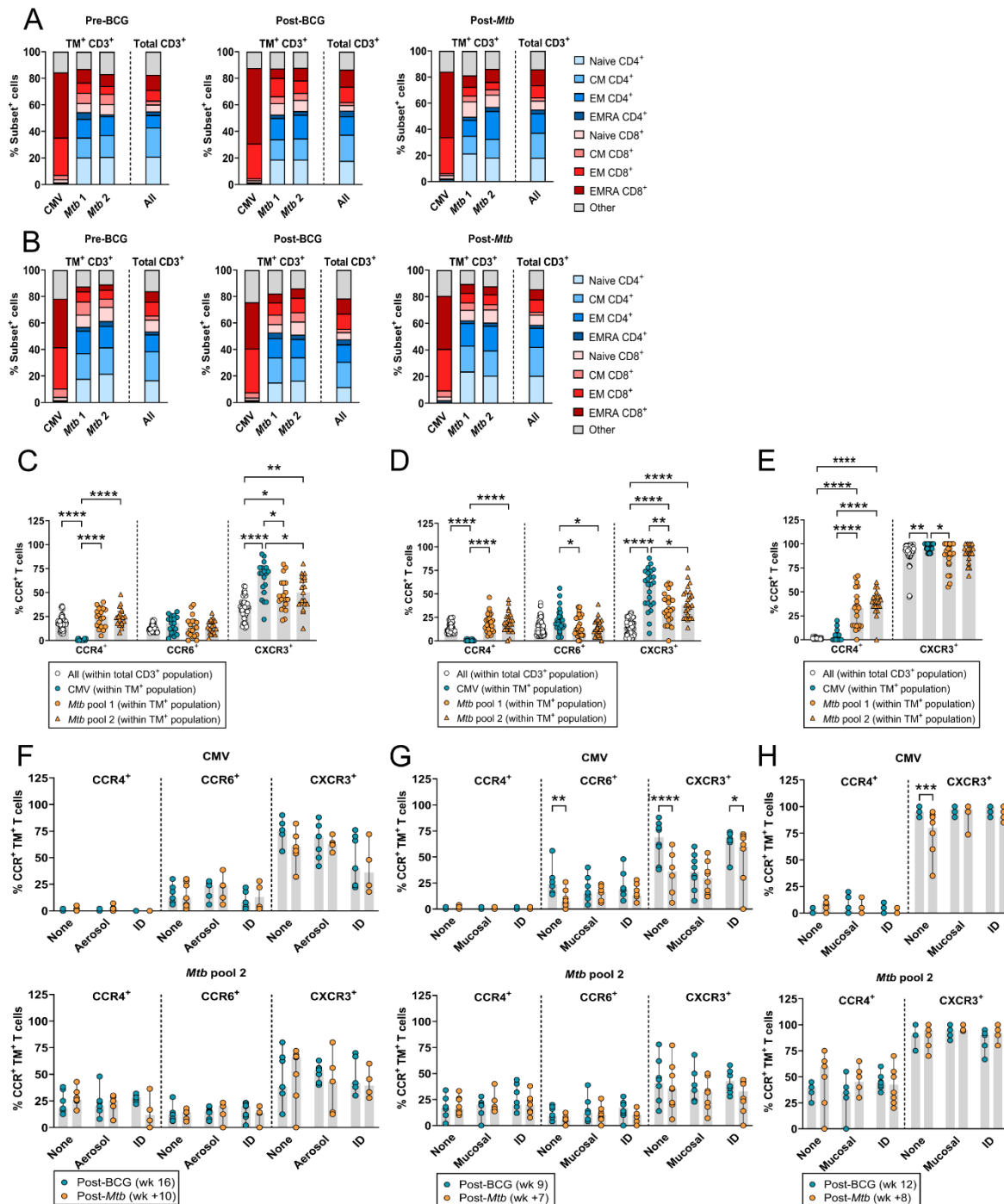
Figure 4. Phenotypic analysis of HLA-E/Mtb CD4+ and CD8+ T cells after BCG vaccination and *Mtb* challenge in RMs. Peptide pools for HLA-E TM staining on RM samples are shown in Table 1. **(A)** Memory subset identification of HLA-E*01:03 *Mtb* and CMV CD3+ T cells relative to total CD3+ T cells in the circulation of RM study 1 (n=19), 4 weeks pre-BCG vaccination (left), 16 weeks post-BCG vaccination (middle) and 10 weeks post-*Mtb* challenge (right); **(B)** Same as A, but then in RM study 2 (n=24) 2 weeks pre-BCG vaccination (left), 9 weeks post-BCG vaccination (middle) and 7 weeks post-*Mtb* challenge (right); **(C)** CCR4, CCR6 and CXCR3 expression on HLA-E*01:03 CMV (blue circles), *Mtb* pool 1 (orange circles) and 2 (orange triangles) CD3+ T cells relative to total CD3+ T cells (white

392   circles) in the circulation 16 weeks post-BCG vaccination in RM study 1 (n=19); **(D)** Same as C, but

393   then for RM study 2 (n=24) 9 weeks post-BCG vaccination; **(E)** Same as D (without CCR6), but then in

394   the BAL 12 weeks post-BCG vaccination; **(F)** CCR4, CCR6 and CXCR3 expression on HLA-E*01:03

395   CMV (upper panel) and *Mtb* pool 2 (lower panel) CD3$^+$ T cells in the circulation 16 weeks post-BCG

396   vaccination (blue) and 10 weeks post-*Mtb* challenge (orange) in RM study 1; **(G)** Same as F, but then

397   for RM study 2, 9 weeks post-BCG vaccination (blue) and 7 weeks post-*Mtb* challenge (orange); **(H)**

398   Same as G, but then in the BAL 12 weeks post-BCG vaccination (blue) and 8 weeks post-*Mtb* challenge

399   (orange). Shaded bars and stacked bars represent the median and mean frequency, respectively, and

400   the error bars represent the 95% confidence interval. Significance was tested using a repeated

401   measures (RM) two-way ANOVA with multiple comparison correction (C – H). * = $p<0.05$, ** = $p<0.01$

402   *** = $p<0.001$, **** = $p<0.0001$.

403

404   *3.5 Simian Immunodeficiency Virus (SIV) co-infection in Mtb-challenged cynomolgus*

405   *macaques and HLA-E/Mtb CD4$^+$ and CD8$^+$ T cell frequencies*

406   Although only three CMs per group, BCG vaccinated, *Mtb* and SIV co-infected CMs tended to

407   have a lower frequency of HLA-E/*Mtb* CD4$^+$ and CD8$^+$ T cells compared to unvaccinated *Mtb*

408   and SIV co-infected CMs, both after *Mtb* and SIV infection (Figure 5A). This was not observed

409   for HLA-E/CMV CD8$^+$ T cells suggesting some level of protection by BCG. HLA-E/*Mtb* and

410   CMV CD4$^+$ and CD8$^+$ T cell frequencies were similar in *Mtb* SIV co-infected and *Mtb* only

411   infected CMs, both in the absence of BCG vaccination, suggesting no effect of SIV co-infection

412   (Figure 5B), and after *Mtb* challenge before SIV infection (Figure 5C), similar to the findings in

413   RMs (Figure 2).
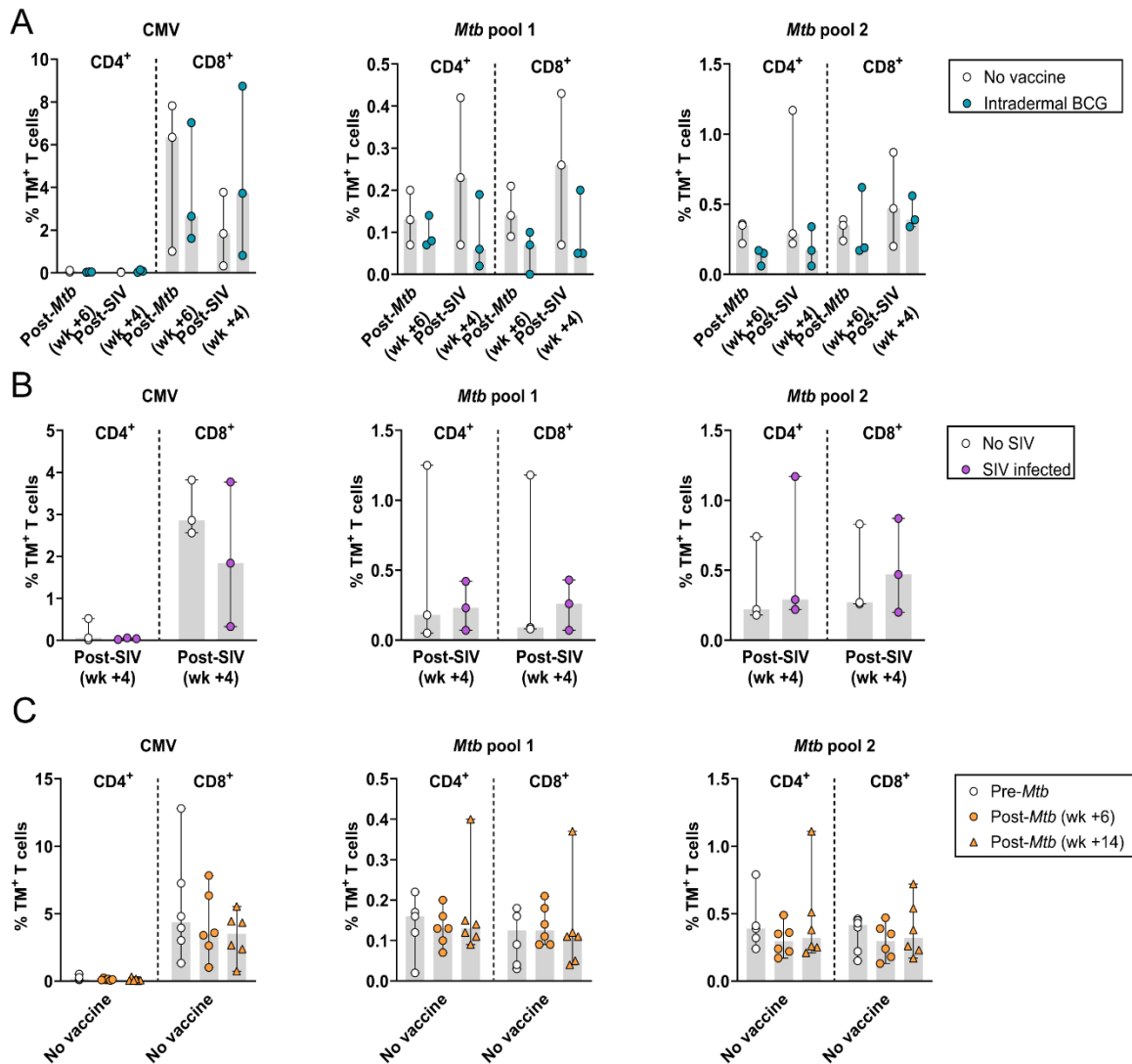
Figure 5. Effect of *Mtb*/SIV co-infection on HLA-E/*Mtb* and CMV CD4+ and CD8+ T cell frequencies in cynomolgus macaques (CMs). Peptide pools for HLA-E TM staining on CM samples are shown in Table 1. 3 CMs were vaccinated with BCG and were challenged with *Mtb* followed by SIV infection, 3 CMs were challenged with *Mtb* followed by SIV infection without BCG vaccination and 3 CMs were challenge with *Mtb* only. **(A)** HLA-E*01:03 CMV (left), *Mtb* pool 1 (middle) and 2 (right) CD4+ and CD8+ T cell frequencies 6 weeks post-*Mtb* challenge and 4 weeks post-SIV challenge in unvaccinated (white) and BCG vaccinated (blue) CMs; **(B)** Same as A, but then 4 weeks post-SIV challenge in unvaccinated and *Mtb* challenged CMs, either without (white) or with (purple) subsequent SIV infection; **(C)** Same as A, but then pre-*Mtb* challenge (white circles) and 6 (orange circles) and 14 weeks (orange triangles) post-*Mtb* challenge (before SIV infection) in six unvaccinated CMs. Shaded bars represent the median frequency, and the error bars represent the 95% confidence interval. Significance was tested using a repeated measures (RM) two-way ANOVA with multiple comparison correction.

4 Discussion

429 We determined HLA-E restricted *Mtb* specific T cell frequencies and their memory phenotypes

430 after BCG vaccination and/or *Mtb* infection in NHPs and in harmonized controlled BCG

431 infection studies in humans. Mucosal and intradermal BCG vaccination did not modulate the

432 frequency of circulating and local HLA-E/*Mtb* CD4⁺ and CD8⁺ T cells in RMs, nor in humans

433 receiving aerosol or intradermal BCG. Previously, intradermal BCG revaccination was found

434 to have no effect on the frequencies of various DURT subsets in the circulation of adults,

435 including MAIT cells, γδ T cells, NKT cells, CD1b and germline-encoded mycolyl-reactive

436 (GEM) T cells[29]. However, γδ T cells were increased after primary vaccination in infants[29].

437 Our findings show that, similar to other DURT subsets, frequencies of HLA-E/*Mtb* restricted T

438 cells were unchanged after BCG revaccination. A previous study showed that intravenous

439 BCG vaccination in RMs induced the highest level of *Mtb* specific T cell responses in the

440 circulation and the BAL and induced the lowest CFU counts compared to intradermal and

441 aerosol. Intravenous BCG might also be more efficient at inducing HLA-E/*Mtb* T cells, though

442 this has to be evaluated in future studies[37]. As the aligned studies in RMs and humans show

443 an almost identical effect of BCG on HLA-E/*Mtb* T cell frequencies, this underscores the

444 relevance of RMs as a model for human mycobacterial infections.

445   *Mtb* challenge significantly increased frequencies of HLA-E/*Mtb* CD3⁺ T cells in the

446 BAL of unvaccinated RMs, suggesting migration to the primary infection site. This increase

447 correlated with higher pathology scores compared to vaccinated RMs, hinting that HLA-E/*Mtb*

448 CD3⁺ T cells might serve as a marker for *Mtb* infection. HLA-E CMV CD3⁺ T cells were

449 detected in the BAL of each RM as well, which is surprising as CMV does not infect the airways

450 like *Mtb*. HLA-E/*Mtb* CD4⁺ and CD8⁺ T cell frequencies remained unchanged in the circulation

451 after *Mtb* challenge in BCG unvaccinated and vaccinated RMs, whereas in active TB and *Mtb*

452 infected humans HLA-E/*Mtb* CD8⁺ T cell frequencies were higher relative to healthy controls,

453 shown previously[13]. Disparities between species, *Mtb* strains and controlled exposure to a

454 defined *Mtb* dose instead of naturally acquiring TB could account for the differences between

455 humans and RMs. The route of administration for mucosal BCG vaccination and *Mtb* challenge

456 in RMs was similar but only *Mtb* increased frequencies of HLA-E/*Mtb* CD4⁺ and CD8⁺ T cells,

457 suggesting that differences in the infection cycle or virulence influenced the capacity to induce

458 HLA-E/*Mtb* restricted T cells.

459   Our findings show that HLA-E CMV TMs were primarily recognized by CD8 expressing

460 T cells, as described earlier[38,39], whereas HLA-E/*Mtb* TMs were recognized by both CD4

461 and CD8 expressing T cells that significantly correlated in both humans and RMs. Future

462 studies should be directed to understand priming of HLA-E restricted T cells, as this likely

463 deviates from conventional T cell priming, both for canonical peptides and especially for HLA-

464   E restricted peptides that are sequentially unrelated to canonical peptides (pathogen-derived),

465   also to establish if co-receptor independent recognition is an HLA-E specific phenomenon.

466   Due to poor staining of the memory markers on BAL samples, the memory phenotype

467   could only be evaluated in PBMCs. Whereas the memory phenotype of circulating HLA-E/*Mtb*

468   CD3$^+$ T cells remained unchanged after BCG vaccination in RMs and BCG infection in humans

469   (Figure S6) and after *Mtb* challenge in RMs, HLA-E CMV CD8$^+$ T cells had an effector memory

470   and terminally differentiated phenotype in RMs, possibly because of prolonged exposure to

471   CMV via circulation in the RM colonies, confirming findings of previous studies[38,40]. The

472   differential CCR expression pattern on HLA-E/*Mtb*, HLA-E/CMV and total T cells might

473   suggest that HLA-E/*Mtb* T cells are more Th2-like T cells and HLA-E/CMV T cells more Th1-

474   like T cells, as described earlier in humans[17,40]. Functional responses, such as the secretion

475   of cytokines, which was not assessed because of limited material availability, should be

476   evaluated for further substantiation.

477   While the frequency of HLA-E/*Mtb* CD4$^+$ and CD8$^+$ T cells was similar between *Mtb*/SIV

478   co-infected and *Mtb* only infected CMs, we previously demonstrated that aTB/HIV co-infected

479   individuals had the highest frequency of HLA-E/*Mtb* CD8$^+$ T cells compared to individuals with

480   aTB and TBI[13]. These individuals were not recently vaccinated with BCG as in CMs and the

481   order of infections as controlled in the CM study was unknown in humans, which could explain

482   the difference between CMs and the previous results on human PBMC samples.

483   Prominent differences were observed between T cells recognizing HLA-E CMV and HLA-

484   E/*Mtb* in terms of frequencies, memory phenotype and co-receptor expression, which

485   precludes that the findings for HLA-E/*Mtb* T cells were merely an effect of non-specific binding

486   or stickiness of the HLA-E/*Mtb* TMs. The frequencies of HLA-E/*Mtb* T cells were low and might

487   have been increased by including more HLA-E/*Mtb* peptides than the four included in this

488   study. It is known that TCR affinity for HLA-E/peptide complexes in general, but especially for

489   peptides that are different to self-peptides, is much lower than for classical HLA-I/peptide

490   complexes, which can also account for the overall low frequencies of HLA-E/*Mtb* T

491   cells[10,14,21]. Furthermore, our results were limited by the number of animals and humans

492   included per study, in particular in the *Mtb*/SIV co-infection study, and the limited material that

493   was available per individual/NHP.

494   In contrast to classical HLA-I molecules, HLA-E is not downregulated by HIV, has limited

495   genetic diversity, can bind to *Mtb* peptides and can be recognized by T cells. These

496   advantages highlight HLA-E's potential as a vaccine target, either to induce *de novo*

497   responses in BCG vaccinated individuals or as a primary vaccine, for example, via vaccination

498   with various immunogenic *Mtb* epitopes in a formulation capable of inducing protective HLA-

499   E restricted T cell responses. Hansen et al. already showed that MHC-E CD8$^+$ T cells were

500   essential to protect against SIV in SIV-infected RMs, but future studies are needed to assess

501   the contribution of HLA-E restricted T cell responses in TB to confirm its efficacy as a primary

502   target[24,41]. Consequently, our study expands current knowledge on the induction of HLA-E

503   restricted T cells after BCG administration and *Mtb* infection and provides new insights into

504   the exploration of HLA-E as a potential protective immune mechanism for TB.

505

506   **Supplementary Materials:** Figure S1: Timelines of the human and NHP studies; Figure S2:

507   Gating strategies to determine HLA-E*01:01 and *01:03 CD4^{+} and CD8^{+} T cell frequencies

508   and their memory phenotype in PBMCs of the human BCG revaccination study (A) and in

509   PBMCs and the BAL of the human BCG infection studies (B-C); Figure S3: Gating strategies

510   to determine HLA-E*01:03 CD4^{+} and CD8^{+} T cell frequencies, chemokine receptor expression

511   and memory phenotype in PBMCs (A) and the BAL (B) of NHP samples in RM studies 1 and

512   2 and in PBMCs from CMs; Figure S4: Representative density plots to determine HLA-E T

513   cells; Figure S5: Data of HLA-E*01:03 T cells for *Mtb* pool 1; Figure S6: Memory phenotype

514   analysis of HLA-E*01:03 *Mtb* CD3^{+} T cells in BCG revaccinated healthy volunteers.

515

516   **Author contributions:** Conceptualization, S.J. and T.O.; methodology, L.V., M.W., A.G., I.S.,

517   J.M., K.D., A.W., S.S., H.S., K.M., T.S.; validation, S.J., T.O., F.W., T.S., S.S. and H.S.; formal

518   analysis, L.V. and M.W.; investigation, L.V., M.W., A.G., I.S., J.M., F.W., K.D., A.W.;

519   resources, A.G., I.S., J.M., F.W., K.F., K.D., A.W., S.S., H.S., T.S.; data curation, L.V., M.W.,

520   I.S., A.G., F.W., A.W., S.S.; writing—original draft preparation, L.V., S.J., K.M., M.W.; writing—

521   review and editing, L.V., S.J., K.M., M.W., T.O., K.F., A.G., T.S., I.S., J.M., K.D., F.W., A.W.,

522   S.S., H.S.; visualization, L.V. and M.W.; supervision, S.J., T.O., T.S., H.S., F.W., S.S.; project

523   administration, S.J., T.O., T.S., H.S., S.S., F.W.; funding acquisition, S.J. and T.O.. All authors

524   have read and agreed to the published version of the manuscript.

525

529

530   **Institutional Review Board Statement:** The human BCG revaccination study was approved

531   by the Medicines Control Council (MCC) of South Africa (now called South African Health

532   Products Regulatory Authority, SAHPRA), by the University Hospital Cleveland Medical

533   Center Institutional Board and the Human Research Ethics Committee of the University of

534   Cape Town (387/2008). The trial protocol of the first BCG controlled human infection study

535   was approved by the Medicines and Healthcare products Regulatory Agency (EudraCT: 2015-

536   004981-27) and the South-Central Oxford A Research Ethics Committee (REC) (15/SC/0716).

537   The trial protocol of the second aerosol BCG infection study was approved by the Central

538   Oxford A REC (18/SC/0307) and is registered in ClinicalTrials.gov (NCT03912207). The first

539   RM study was approved by the UK Health Security Agency Animal Welfare and Ethical Review

540   Body and was authorised under UK Home Office Licence P219D8D1A. The study protocol of

541   the second RM study approved by the independent ethics committee Dier Experimenten

542   Commissie (DEC) (761subB) and the institutional animal welfare body of the Biomedical

543   Primate Research Center (BPRC). The CM study design and animal housing was approved

544   by the Establishment Animal Welfare and Ethical Review Committee and authorised under

545   UK Home Office Project License P219D8D1A.

546

547   **Informed Consent Statement:** Informed consent was obtained from all individuals involved

548   in the study.

549

550   **Data Availability Statement:** The original contributions presented in the study are included

551   in the article/supplementary material, further inquiries can be directed to the corresponding

552   author.

553

557

558   **Conflicts of interest:** The authors declare no conflicts of interest.

559

560   **References**

561   1.   Global tuberculosis report 2023. *Geneva: World Health Organization* **2023**.

562   2.   Hunter, R.L.; Actor, J.K.; Hwang, S.A.; Khan, A.; Urbanowski, M.E.; Kaushal, D.;
563   Jagannath, C. Pathogenesis and Animal Models of Post-Primary (Bronchogenic)
564   Tuberculosis, A Review. *Pathogens* **2018**, *7*, doi:10.3390/pathogens7010019.

565   3.   Cardona, P.J.; Williams, A. Experimental animal modelling for TB vaccine
566   development. *Int J Infect Dis* **2017**, *56*, 268-273, doi:10.1016/j.ijid.2017.01.030.

567   4.   Ruibal, P.; Voogd, L.; Joosten, S.A.; Ottenhoff, T.H.M. The role of donor-unrestricted
568   T-cells, innate lymphoid cells, and NK cells in anti-mycobacterial immunity. *Immunol*
569   *Rev* **2021**, *301*, 30-47, doi:10.1111/imr.12948.

570   5.   Kanevskiy, L.; Erokhina, S.; Kobyzeva, P.; Streltsova, M.; Sapozhnikov, A.; Kovalenko,
571   E. Dimorphism of HLA-E and its Disease Association. *Int J Mol Sci* **2019**, *20*,
572   doi:10.3390/ijms20215496.

6. Strong, R.K.; Holmes, M.A.; Li, P.; Braun, L.; Lee, N.; Geraghty, D.E. HLA-E allelic variants. Correlating differential expression, peptide affinities, crystal structures, and thermal stabilities. *J Biol Chem* **2003**, *278*, 5082-5090, doi:10.1074/jbc.M208268200.

7. Lee, N.; Llano, M.; Carretero, M.; Ishitani, A.; Navarro, F.; Lopez-Botet, M.; Geraghty, D.E. HLA-E is a major ligand for the natural killer inhibitory receptor CD94/NKG2A. *Proc Natl Acad Sci U S A* **1998**, *95*, 5199-5204, doi:10.1073/pnas.95.9.5199.

8. Braud, V.M.; Allan, D.S.; O'Callaghan, C.A.; Soderstrom, K.; D'Andrea, A.; Ogg, G.S.; Lazetic, S.; Young, N.T.; Bell, J.I.; Phillips, J.H.; et al. HLA-E binds to natural killer cell receptors CD94/NKG2A, B and C. *Nature* **1998**, *391*, 795-799, doi:10.1038/35869.

9. Voogd, L.; Ruibal, P.; Ottenhoff, T.H.M.; Joosten, S.A. Antigen presentation by MHC-E: a putative target for vaccination? *Trends Immunol* **2022**, *43*, 355-365, doi:10.1016/j.it.2022.03.002.

10. Voogd, L.; Drittij, A.; Dingenouts, C.K.E.; Franken, K.; Unen, V.V.; van Meijgaarden, K.E.; Ruibal, P.; Hagedoorn, R.S.; Leitner, J.A.; Steinberger, P.; et al. Mtb HLA-E-tetramer-sorted CD8(+) T cells have a diverse TCR repertoire. *iScience* **2024**, *27*, 109233, doi:10.1016/j.isci.2024.109233.

11. Ruibal, P.; Franken, K.; van Meijgaarden, K.E.; van Wolfswinkel, M.; Derksen, I.; Scheeren, F.A.; Janssen, G.M.C.; van Veelen, P.A.; Sarfas, C.; White, A.D.; et al. Identification of HLA-E Binding Mycobacterium tuberculosis-Derived Epitopes through Improved Prediction Models. *J Immunol* **2022**, *209*, 1555-1565, doi:10.4049/jimmunol.2200122.

12. Ruibal, P.; Derksen, I.; van Wolfswinkel, M.; Voogd, L.; Franken, K.; El Hebieshy, A.F.; van Hall, T.; Schoufour, T.A.W.; Wijdeven, R.H.; Ottenhoff, T.H.M.; et al. Thermal-exchange HLA-E multimers reveal specificity in HLA-E and NKG2A/CD94 complex interactions. *Immunology* **2023**, *168*, 526-537, doi:10.1111/imm.13591.

13. Prezzemolo, T.; van Meijgaarden, K.E.; Franken, K.; Caccamo, N.; Dieli, F.; Ottenhoff, T.H.M.; Joosten, S.A. Detailed characterization of human Mycobacterium tuberculosis specific HLA-E restricted CD8(+) T cells. *Eur J Immunol* **2018**, *48*, 293-305, doi:10.1002/eji.201747184.

14. Yang, H.; Sun, H.; Brackenridge, S.; Zhuang, X.; Wing, P.A.C.; Quastel, M.; Walters, L.; Garner, L.; Wang, B.; Yao, X.; et al. HLA-E-restricted SARS-CoV-2-specific T cells from convalescent COVID-19 patients suppress virus replication despite HLA class Ia down-regulation. *Sci Immunol* **2023**, *8*, eabl8881, doi:10.1126/sciimmunol.abl8881.

15. Salerno-Goncalves, R.; Fernandez-Vina, M.; Lewinsohn, D.M.; Sztein, M.B. Identification of a human HLA-E-restricted CD8+ T cell subset in volunteers immunized with Salmonella enterica serovar Typhi strain Ty21a typhoid vaccine. *J Immunol* **2004**, *173*, 5852-5862, doi:10.4049/jimmunol.173.9.5852.

16. Vietzen, H.; Furlano, P.L.; Cornelissen, J.J.; Bohmig, G.A.; Jaksch, P.; Puchhammer-Stockl, E. HLA-E-restricted immune responses are crucial for the control of EBV infections and the prevention of PTLD. *Blood* **2023**, *141*, 1560-1573, doi:10.1182/blood.2022017650.

17. van Meijgaarden, K.E.; Haks, M.C.; Caccamo, N.; Dieli, F.; Ottenhoff, T.H.; Joosten, S.A. Human CD8+ T-cells recognizing peptides from Mycobacterium tuberculosis (Mtb) presented by HLA-E have an unorthodox Th2-like, multifunctional, Mtb inhibitory phenotype and represent a novel human T-cell subset. *PLoS Pathog* **2015**, *11*, e1004671, doi:10.1371/journal.ppat.1004671.

18. Joosten, S.A.; van Meijgaarden, K.E.; van Weeren, P.C.; Kazi, F.; Geluk, A.; Savage, N.D.; Drijfhout, J.W.; Flower, D.R.; Hanekom, W.A.; Klein, M.R.; et al. Mycobacterium tuberculosis peptides presented by HLA-E molecules are targets for human CD8 T-cells with cytotoxic as well as regulatory activity. *PLoS Pathog* **2010**, *6*, e1000782, doi:10.1371/journal.ppat.1000782.

19. Doorduijn, E.M.; Sluijter, M.; Marijt, K.A.; Querido, B.J.; van der Burg, S.H.; van Hall, T. T cells specific for a TAP-independent self-peptide remain naive in tumor-bearing mice and are fully exploitable for therapy. *Oncoimmunology* **2018**, *7*, e1382793, doi:10.1080/2162402X.2017.1382793.

20. Doorduijn, E.M.; Sluijter, M.; Querido, B.J.; Seidel, U.J.E.; Oliveira, C.C.; van der Burg, S.H.; van Hall, T. T Cells Engaging the Conserved MHC Class Ib Molecule Qa-1(b) with TAP-Independent Peptides Are Semi-Invariant Lymphocytes. *Front Immunol* **2018**, *9*, 60, doi:10.3389/fimmu.2018.00060.

21. Yang, H.; Rei, M.; Brackenridge, S.; Brenna, E.; Sun, H.; Abdulhaqq, S.; Liu, M.K.P.; Ma, W.; Kurupati, P.; Xu, X.; et al. HLA-E-restricted, Gag-specific CD8(+) T cells can suppress HIV-1 infection, offering vaccine opportunities. *Sci Immunol* **2021**, *6*, doi:10.1126/sciimmunol.abg1703.

22. Jorgensen, P.B.; Livbjerg, A.H.; Hansen, H.J.; Petersen, T.; Hollsberg, P. Epstein-Barr virus peptide presented by HLA-E is predominantly recognized by CD8(bright) cells in multiple sclerosis patients. *PLoS One* **2012**, *7*, e46120, doi:10.1371/journal.pone.0046120.

23. Bian, Y.; Shang, S.; Siddiqui, S.; Zhao, J.; Joosten, S.A.; Ottenhoff, T.H.M.; Cantor, H.; Wang, C.R. MHC Ib molecule Qa-1 presents Mycobacterium tuberculosis peptide antigens to CD8+ T cells and contributes to protection against infection. *PLoS Pathog* **2017**, *13*, e1006384, doi:10.1371/journal.ppat.1006384.

24. Hansen, S.G.; Marshall, E.E.; Malouli, D.; Ventura, A.B.; Hughes, C.M.; Ainslie, E.; Ford, J.C.; Morrow, D.; Gilbride, R.M.; Bae, J.Y.; et al. A live-attenuated RhCMV/SIV

646   vaccine shows long-term efficacy against heterologous SIV challenge. *Sci Transl Med*
647   **2019**, *11*, doi:10.1126/scitranslmed.aaw2607.

648 25. Malouli, D.; Gilbride, R.M.; Wu, H.L.; Hwang, J.M.; Maier, N.; Hughes, C.M.;
649   Newhouse, D.; Morrow, D.; Ventura, A.B.; Law, L.; et al. Cytomegalovirus-vaccine-
650   induced unconventional T cell priming and control of SIV replication is conserved
651   between primate species. *Cell Host Microbe* **2022**, *30*, 1207-1218 e1207,
652   doi:10.1016/j.chom.2022.07.013.

653 26. Verweij, M.C.; Hansen, S.G.; Iyer, R.; John, N.; Malouli, D.; Morrow, D.; Scholz, I.;
654   Womack, J.; Abdulhaqq, S.; Gilbride, R.M.; et al. Modulation of MHC-E transport by
655   viral decoy ligands is required for RhCMV/SIV vaccine efficacy. *Science* **2021**, *372*,
656   doi:10.1126/science.abe9233.

657 27. Nattermann, J.; Nischalke, H.D.; Hofmeister, V.; Kupfer, B.; Ahlenstiel, G.; Feldmann,
658   G.; Rockstroh, J.; Weiss, E.H.; Sauerbruch, T.; Spengler, U. HIV-1 infection leads to
659   increased HLA-E expression resulting in impaired function of natural killer cells. *Antivir*
660   *Ther* **2005**, *10*, 95-107, doi:10.1177/135965350501000107.

661 28. Ruibal, P.; Franken, K.; van Meijgaarden, K.E.; Walters, L.C.; McMichael, A.J.;
662   Gillespie, G.M.; Joosten, S.A.; Ottenhoff, T.H.M. Discovery of HLA-E-Presented
663   Epitopes: MHC-E/Peptide Binding and T-Cell Recognition. *Methods Mol Biol* **2022**,
664   *2574*, 15-30, doi:10.1007/978-1-0716-2712-9_2.

665 29. Gela, A.; Murphy, M.; Rodo, M.; Hadley, K.; Hanekom, W.A.; Boom, W.H.; Johnson,
666   J.L.; Hoft, D.F.; Joosten, S.A.; Ottenhoff, T.H.M.; et al. Effects of BCG vaccination on
667   donor unrestricted T cells in two prospective cohort studies. *EBioMedicine* **2022**, *76*,
668   103839, doi:10.1016/j.ebiom.2022.103839.

669 30. Hatherill, M.; Geldenhuys, H.; Pienaar, B.; Suliman, S.; Chheng, P.; Debanne, S.M.;
670   Hoft, D.F.; Boom, W.H.; Hanekom, W.A.; Johnson, J.L. Safety and reactogenicity of
671   BCG revaccination with isoniazid pretreatment in TST positive adults. *Vaccine* **2014**,
672   *32*, 3982-3988, doi:10.1016/j.vaccine.2014.04.084.

673 31. Satti, I.; Marshall, J.L.; Harris, S.A.; Wittenberg, R.; Tanner, R.; Lopez Ramon, R.;
674   Wilkie, M.; Ramos Lopez, F.; Riste, M.; Wright, D.; et al. Safety of a controlled human
675   infection model of tuberculosis with aerosolised, live-attenuated Mycobacterium bovis
676   BCG versus intradermal BCG in BCG-naive adults in the UK: a dose-escalation,
677   randomised, controlled, phase 1 trial. *Lancet Infect Dis* **2024**, doi:10.1016/S1473-
678   3099(24)00143-9.

679 32. White, A.D.; Sarfas, C.; Sibley, L.S.; Gullick, J.; Clark, S.; Rayner, E.; Gleeson, F.;
680   Catala, M.; Nogueira, I.; Cardona, P.J.; et al. Protective Efficacy of Inhaled BCG
681   Vaccination Against Ultra-Low Dose Aerosol M. tuberculosis Challenge in Rhesus
682   Macaques. *Pharmaceutics* **2020**, *12*, doi:10.3390/pharmaceutics12050394.

683   33.   Dijkman, K.; Sombroek, C.C.; Vervenne, R.A.W.; Hofman, S.O.; Boot, C.; Remarque,
684   E.J.; Kocken, C.H.M.; Ottenhoff, T.H.M.; Kondova, I.; Khayum, M.A.; et al. Prevention
685   of tuberculosis infection and disease by local BCG in repeatedly exposed rhesus
686   macaques. *Nat Med* **2019**, *25*, 255-262, doi:10.1038/s41591-018-0319-9.
687   34.   White, A.D.; Sibley, L.; Gullick, J.; Sarfas, C.; Clark, S.; Fagrouch, Z.; Verschoor, E.;
688   Salguero, F.J.; Dennis, M.; Sharpe, S. TB and SIV Coinfection; a Model for Evaluating
689   Vaccine Strategies against TB Reactivation in Asian Origin Cynomolgus Macaques: A
690   Pilot   Study   Using   BCG   Vaccination. *Vaccines   (Basel)*   **2021**,   *9*,
691   doi:10.3390/vaccines9090945.
692   35.   van Wolfswinkel, M.; van Meijgaarden, K.E.; Ottenhoff, T.H.M.; Niewold, P.; Joosten,
693   S.A. Extensive flow cytometric immunophenotyping of human PBMC incorporating
694   detection of chemokine receptors, cytokines and tetramers. *Cytometry A* **2023**, *103*,
695   600-610, doi:10.1002/cyto.a.24727.
696   36.   Walters, L.C.; Harlos, K.; Brackenridge, S.; Rozbesky, D.; Barrett, J.R.; Jain, V.;
697   Walter, T.S.; O'Callaghan, C.A.; Borrow, P.; Toebes, M.; et al. Pathogen-derived HLA-
698   E bound epitopes reveal broad primary anchor pocket tolerability and conformationally
699   malleable peptide binding. *Nat Commun* **2018**, *9*, 3137, doi:10.1038/s41467-018-
700   05459-z.
701   37.   Darrah, P.A.; Zeppa, J.J.; Maiello, P.; Hackney, J.A.; Wadsworth, M.H., 2nd; Hughes,
702   T.K.; Pokkali, S.; Swanson, P.A., 2nd; Grant, N.L.; Rodgers, M.A.; et al. Prevention of
703   tuberculosis in macaques after intravenous BCG immunization. *Nature* **2020**, *577*, 95-
704   102, doi:10.1038/s41586-019-1817-8.
705   38.   Sullivan, L.C.; Westall, G.P.; Widjaja, J.M.; Mifsud, N.A.; Nguyen, T.H.; Meehan, A.C.;
706   Kotsimbos, T.C.; Brooks, A.G. The Presence of HLA-E-Restricted, CMV-Specific
707   CD8+ T Cells in the Blood of Lung Transplant Recipients Correlates with Chronic
708   Allograft   Rejection. *PLoS   One*   **2015**,   *10*,   e0135972,
709   doi:10.1371/journal.pone.0135972.
710   39.   Pietra, G.; Romagnani, C.; Mazzarino, P.; Falco, M.; Millo, E.; Moretta, A.; Moretta, L.;
711   Mingari, M.C. HLA-E-restricted recognition of cytomegalovirus-derived peptides by
712   human CD8+ cytolytic T lymphocytes. *Proc Natl Acad Sci U S A* **2003**, *100*, 10896-
713   10901, doi:10.1073/pnas.1834449100.
714   40.   Mazzarino, P.; Pietra, G.; Vacca, P.; Falco, M.; Colau, D.; Coulie, P.; Moretta, L.;
715   Mingari, M.C. Identification of effector-memory CMV-specific T lymphocytes that kill
716   CMV-infected target cells in an HLA-E-restricted fashion. *Eur J Immunol* **2005**, *35*,
717   3240-3247, doi:10.1002/eji.200535343.
718   41.   Hansen, S.G.; Wu, H.L.; Burwitz, B.J.; Hughes, C.M.; Hammond, K.B.; Ventura, A.B.;
719   Reed, J.S.; Gilbride, R.M.; Ainslie, E.; Morrow, D.W.; et al. Broadly targeted CD8(+) T

720   cell responses restricted by major histocompatibility complex E. *Science* **2016**, *351*,

721   714-720, doi:10.1126/science.aac9475.

722

723   **Disclaimer/Publisher's Note:** The statements, opinions and data contained in all publications

724   are solely those of the individual author(s) and contributor(s) and not of MDPI and/or the

725   editor(s). MDPI and/or the editor(s) disclaim responsibility for any in-jury to people or property

726   resulting from any ideas, methods, instructions or products referred to in the content.

727

728

729

730

731

732

733

734

735

736

737

738

739

740

741

742

743

744

745

746

747

748

749

750

751

752

753

754

755

756 **Supplementary Materials**
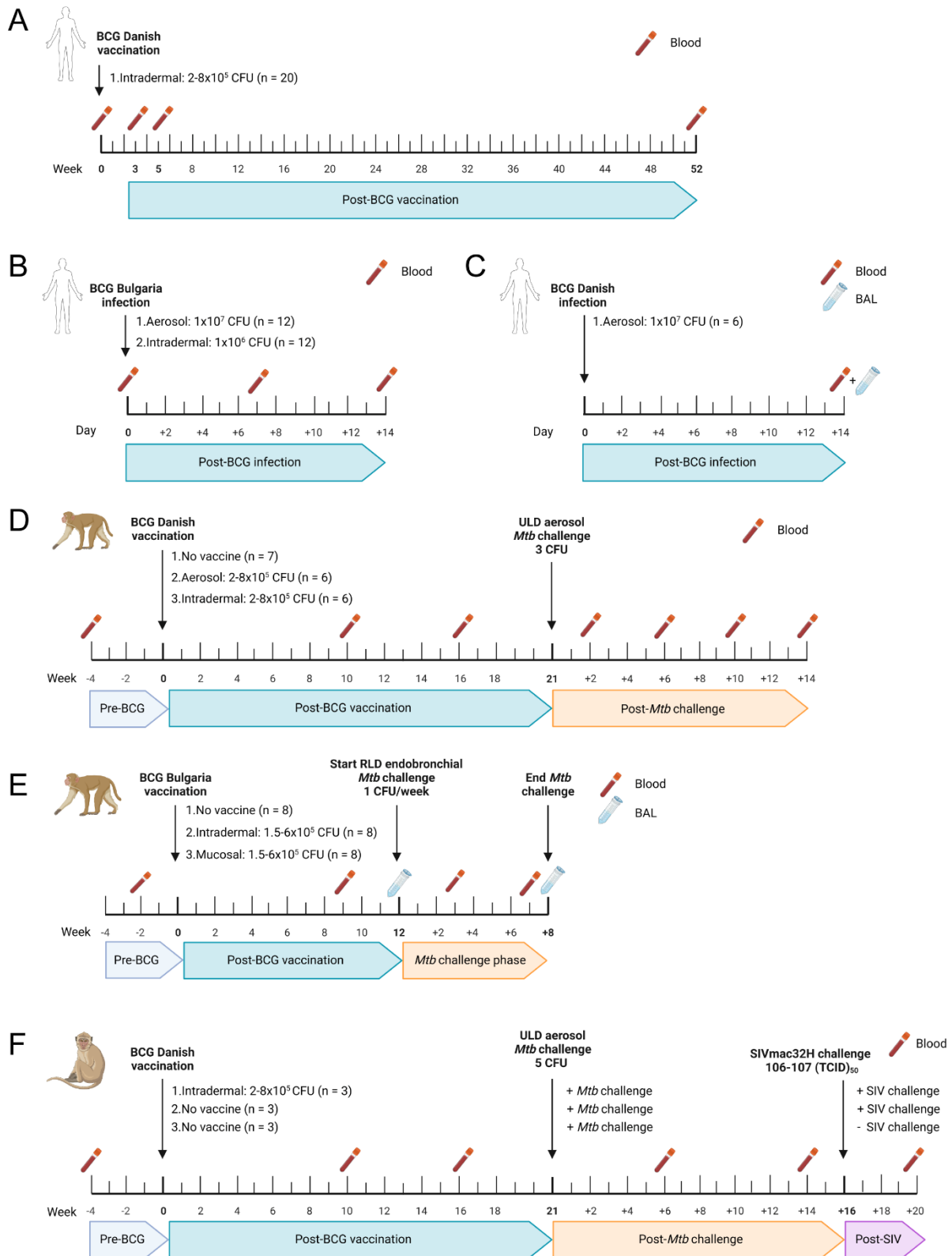
757

758 **Figure S 1.** Timelines of the human and NHP studies. Timeline of the human BCG revaccination study.

759 Blood was collected at indicated timepoints; **(A)** Timeline of the controlled human BCG infection study

760 1. Blood was collected at indicated timepoints; **(B)** Timeline of the controlled human BCG infection study

761   2. Blood and BAL were collected at indicated timepoints; **(C)** Timeline of BCG vaccination and *Mtb*

762   challenge in RM study 1. Blood was collected at indicated timepoints; **(D)** Timeline of BCG vaccination

763   and *Mtb* challenge in RM study 2. Blood and BAL were collected at indicated timepoints; **(E)** Timeline

764   of BCG vaccination, *Mtb* challenge and SIV infection in the CM study. Blood was collected at indicated

765   timepoints.

766
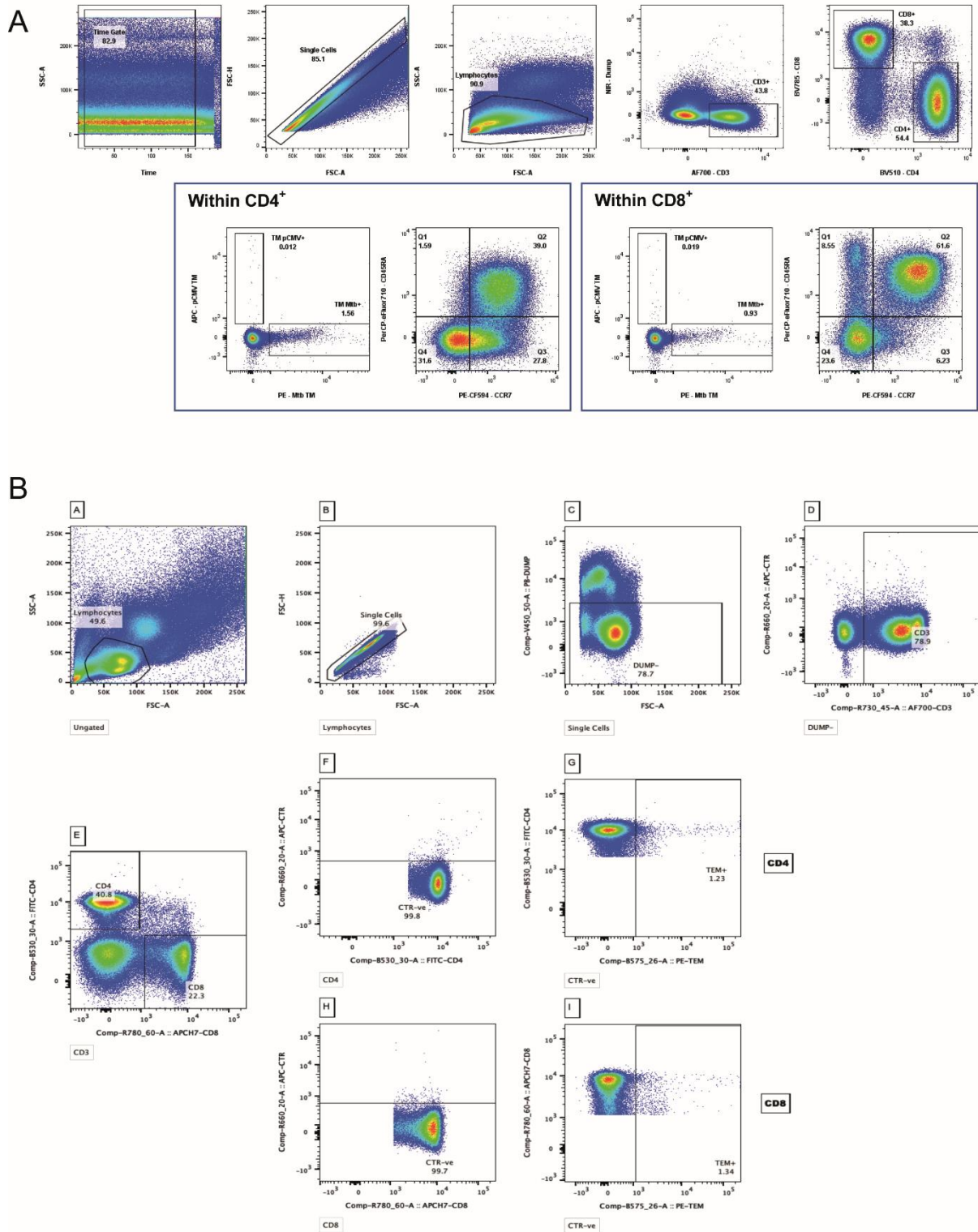
Figure S 2. Gating strategies to determine HLA-E*01:01 and *01:03 CD4+ and CD8+ T cell frequencies and their memory phenotype in PBMCs of the human BCG revaccination study (A) and in PBMCs and BAL of the human BCG infection studies (B).
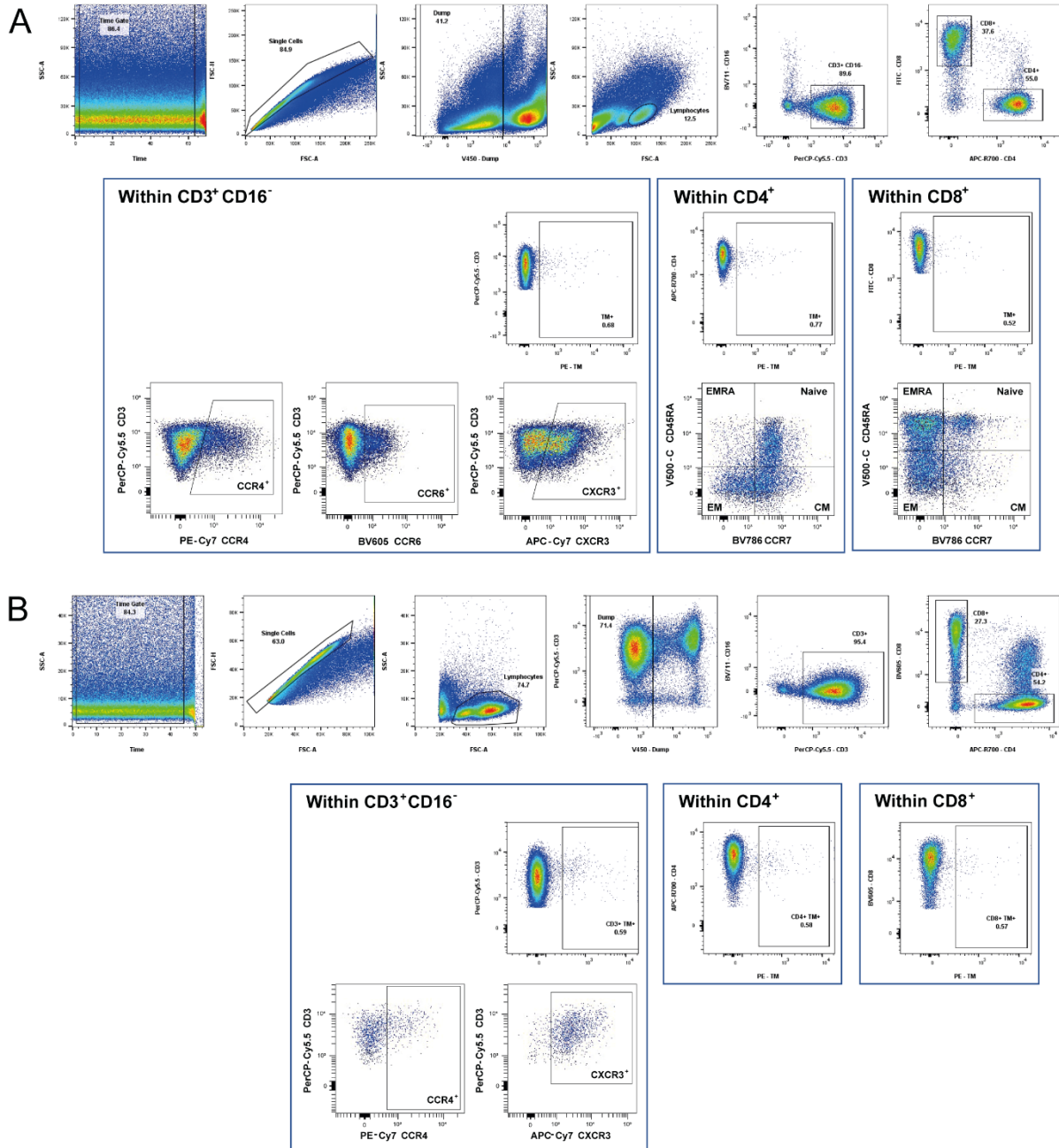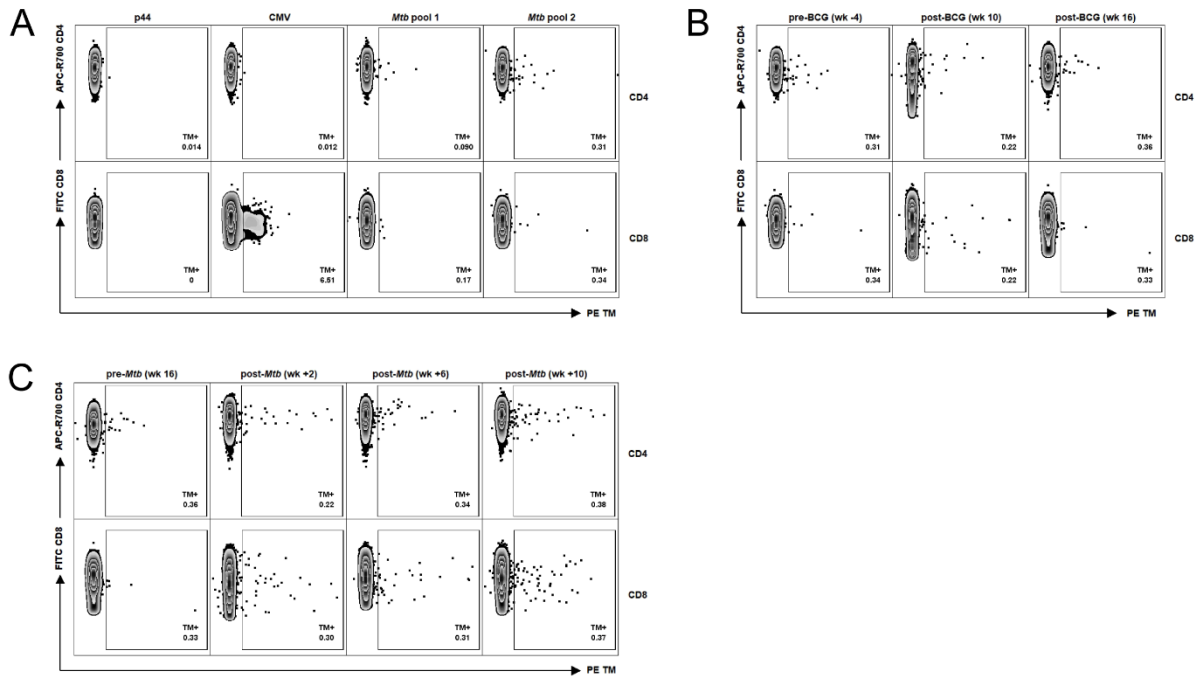
770

771

772 **Figure S 3.** Gating strategies to determine HLA-E*01:03 CD4+ and CD8+ T cell frequencies, chemokine
773 receptor expression and memory phenotype in PBMCs (A) and BAL (B) of NHP samples in RM studies
774 1 and 2 and in PBMCs from CMs.

Figure S 4. Representative density plots to determine HLA-E T cells. Peptide pools for HLA-E TM staining on RM samples are shown in Table 1. **(A)** Representative density plots for p44, CMV and *Mtb* pool 1 and 2 HLA-E*01:03 CD4+ and CD8+ T cell frequencies in one aerosol BCG vaccinated RM of study 1 at the pre-vaccination time point; **(B)** Representative density plots for *Mtb* pool 2 HLA-E*01:03 CD4+ and CD8+ T cell frequencies at the pre-vaccination time point and 10 and 16 weeks post-BCG vaccination in one aerosol vaccinated RM of study 1; **(C)** Representative density plots for *Mtb* pool 2 HLA-E*01:03 CD4+ and CD8+ T cell frequencies, 16 weeks post-BCG vaccination and 2, 6 and 10 weeks post-*Mtb* challenge in one aerosol vaccinated RM of study 1. In A-C, HLA-E TMs labelled with PE are shown on the X-axis and CD4 and CD8 are shown on the Y-axis.
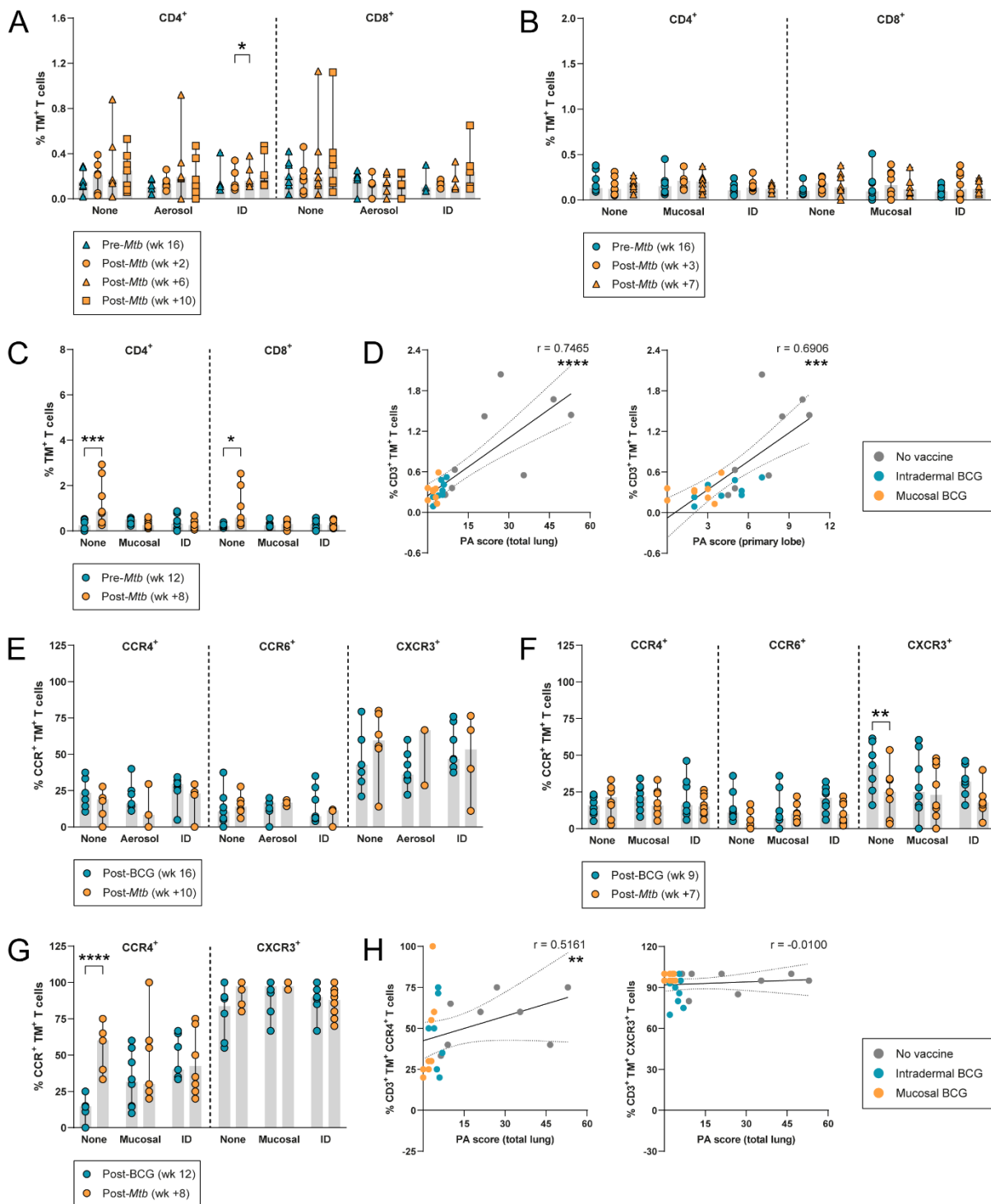
Figure S 5. Data of HLA-E*01:03 T cells for *Mtb* pool 1. Peptides and sequences for HLA-E TM staining with *Mtb* pool 1 on RM samples are shown in Table 1. **(A)** HLA-E*01:03 CD4+ and CD8+ T cell frequencies in RM study 1 at the pre-*Mtb* challenge time point (blue triangles) and 2 (orange circles), 6 (orange triangles) and 10 weeks (orange squares) post-*Mtb* challenge; **(B)** Same as A, but then for RM study 2 at the pre-*Mtb* challenge time point (blue circles) and 3 and 7 weeks (orange circles and orange triangles) post-*Mtb* challenge; **(C)** HLA-E*01:03 CD4+ and CD8+ T cell frequencies in BAL of RM study 2 at the post-BCG vaccination time point (blue) and the post-*Mtb* challenge time point (orange); **(D)** Correlating the frequency of HLA-E*01:03 CD3+ T cells in BAL (Y-axis) and the PA scores in the total

794   lung (left) and primary lobe (right) (X-axis) of RM study 2. Grey dots represent the unvaccinated group,

795   blue dots the intradermal BCG vaccinated group and orange dots the mucosal BCG vaccinated group.

796   Dotted lines represent the 95% confidence interval; **(E)** CCR4, CCR6 and CXCR3 expression on HLA-

797   E*01:03 CD3$^+$ T cells in RM study 1, 16 weeks post-BCG vaccination (blue) and 10 weeks post-*Mtb*

798   challenge (orange); **(F)** Same as E, but then for RM study 2, 9 weeks post-BCG vaccination (blue) and

799   7 weeks post-*Mtb* challenge (orange); **(G)** Same as F (without CCR6), but then in BAL 12 weeks post-

800   BCG vaccination (blue) and 8 weeks post-*Mtb* challenge (orange); **(H)** Correlating the frequency of

801   CCR4$^+$ (left) and CXCR3$^+$ (right) HLA-E*01:03 CD3$^+$ T cells in BAL on the Y-axis and the PA scores in

802   the total lung on the X-axis, 8 weeks post-*Mtb* challenge in RM study 2. Grey dots represent the

803   unvaccinated group, blue dots the intradermal BCG vaccinated group and orange dots the mucosal

804   BCG vaccinated group. Dotted lines represent the 95% confidence interval. Shaded bars represent the

805   median frequency and the error bars represent the 95% confidence interval. Significance was tested

806   using a repeated measures (RM) two-way ANOVA with multiple comparison correction (A – C, E – G)

807   and a Spearman's rank correlation (D, H). * = $p<0.05$, ** = $p<0.01$ *** = $p<0.001$, **** = $p<0.0001$.

808
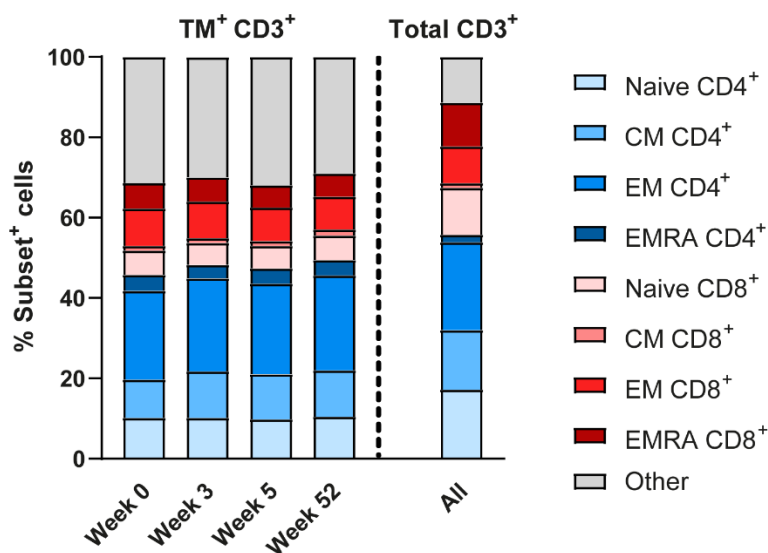
809

810   **Figure S 6.** Memory phenotype analysis of HLA-E*01:03 *Mtb* CD3$^+$ T cells in BCG revaccinated healthy

811   volunteers. Peptides and sequences for HLA-E TM staining with the *Mtb* pool on human samples are

812   shown in Table 1. Memory subset identification of HLA-E*01:03 CD3$^+$ T cells for the *Mtb* pool relative

813   to total CD3$^+$ T cells in BCG revaccinated human volunteers (n=20) 0, 3, 5 and 52 weeks post-BCG

814   revaccination relative to total CD3$^+$ T cells. Stacked bars show the mean frequency.